ASIATIC ACID LOADED PVA EMULSIFIED PLGA NANOPARTICLES: FORMULATION, PHYSICOCHEMICAL CHARACTERIZATION & IN VITRO RELEASE STUDY

THESIS SUBMITTED IN PARTIAL FULFILLMENT OF THE REQUIREMENTS OF THE DEGREE OF
MASTER OF PHARMACY
(2019)

SUBMITTED
BY
MS. SUSMITA BASAK
CLASS ROLL NUMBER: 001711402027
EXAMINATION ROLL NUMBER: M4PHA19027
REGISTRATION NUMBER: 140851 of 2017-18

UNDER THE GUIDANCE
OF
DR. SAIKAT DEWANJEE

DEPARTMENT OF PHARMACEUTICAL TECHNOLOGY
FACULTY OF ENGINEERING AND TECHNOLOGY
JADAVPUR UNIVERSITY
KOLKATA- 700032
INDIA

ASIATIC ACID LOADED PVA EMULSIFIED PLGA NANOPARTICLES: FORMULATION, PHYSICOCHEMICAL CHARACTERIZATION & IN VITRO RELEASE STUDY

THESIS SUBMITTED IN PARTIAL FULFILLMENT OF THE REQUIREMENTS OF THE DEGREE OF
MASTER OF PHARMACY
(2019)

SUBMITTED
BY
MS. SUSMITA BASAK
CLASS ROLL NUMBER: 001711402027
EXAMINATION ROLL NUMBER: M4PHA19027
REGISTRATION NUMBER: 140851 of 2017-18

UNDER THE GUIDANCE
OF
DR. SAIKAT DEWANJEE

DEPARTMENT OF PHARMACEUTICAL TECHNOLOGY
FACULTY OF ENGINEERING AND TECHNOLOGY
JADAVPUR UNIVERSITY
KOLKATA- 700032
INDIA

Certificate of Approval

This is to certify that the term paper entitled **"Asiatic Acid Loaded PVA Emulsified PLGA Nanoparticles: Formulation, Physicochemical Characterization & In Vitro Release Study"** has been carried out by **Ms. Susmita Basak** under my supervision at Department of Pharmaceutical Technology, Jadavpur University, Kolkata-700032, in the partial fulfilment of the requirements for the degree of **"Master of Pharmacy"** of this university.

_____

DR. SAIKAT DEWANJEE
Project supervisor and Assistant Professor
Department of Pharmaceutical Technology
Faculty of Engineering and Technology
Jadavpur University
Kolkata 700032, India

_____

PROF. PULOK K. MUKHERJEE
Head of the Department
Department of Pharmaceutical Technology
Faculty of Engineering and Technology
Jadavpur University
Kolkata 700032, India

_____

PROF. CHIRANJIB BHATTACHARJEE
Dean, Faculty of Engineering and Technology
Jadavpur University
Kolkata 700032, India

DECLARATION OF ORIGINALITY AND COMPLIANCE OF ACADEMIC ETHICS

I, Susmita Basak, hereby declare that the thesis contains literature survey and original research work pursed by me. As a part of my thesis work entitled **"Asiatic Acid Loaded PVA Emulsified PLGA Nanoparticles: Formulation, Physicochemical Characterization & In Vitro Release Study"**.

All the information in this document have obtained and presented in accordance with academic rules and ethical conduct.

I also declare that as required by thesis rules and conduct, I have fully cited and referenced all the materials and results that are not original to this work.

Name: Ms. Susmita Basak

Examination Roll No: M4PHA19027

Registration No: 140851 of 2017-18

Thesis title: **"Asiatic Acid Loaded PVA Emulsified PLGA Nanoparticles: Formulation, Physicochemical Characterization & In Vitro Release Study".**

Place:

Date: ……

Ms. Susmita Basak

ACKNOWLEDGEMENTS

It gives a great pleasure to acknowledge my immense respect and depth of gratitude to my esteemed guide ***Dr. Saikat Dewanjee****, who has been a constant source of encouragement and treasure of valuable inspiring guidance. His kind nature, disciplined technical advice, uncompromising commitment and perfection throughout the work offered me great interest and courage to sustain the efforts to complete my project.*

I would like to express my gratitude to my co-supervisor ***Prof. Biswajit Mukherjee*** *for providing me knowledge and guidelines to carry out the project work.*

I would like to express my gratitude to ***Prof. Pulok Kumar Mukherjee****, Head, Department of Pharmaceutical Technology for his kind support.*

I extend my whole hearted thanks to my seniors Mr. Samrat Chakraborty, Dr. Tarun Kumar Dua, Dr. Paramita Paul Dua, Dr. Ranabir Sahu, Ms. Swarnalata Joardar, Mr. Sojit Das, Mr. Pratik Chakraborty, Ms. Apala Chakraborty, Mr. Ashique Al Hoque, Mr. Brahamacharry Paul and my dear friends Sanchari, Ajeya, Deepayan, Shounak, Sahajit.

I would like to express my special thanks to each and every members of Advanced Pharmacognosy Research Laboratory, Department of Pharmaceutical Technology, Jadavpur University who were always with me during my project work.

I would like to express my gratitude to School of Materials Science & Nanotechnology, Jadavpur University, Indian Institute of Chemical Biology, Indian Association for the Cultivation of Science, S.N. Bose National Centre For Basic Sciences, and Bose Institute, Kolkata for their assistance.

Thanks to all my teachers, friends, relatives and acquaintances who don't find a mention here, but to whom I will always be thankful from the core of my heart.

Finally, it is impossible for me to express my gratitude to my father ***Mr. Jagabandhu Basak****, my mother* ***Mrs. Durga Basak****, my elder brother, and my grandmother in words. Their unconditional love, blessings and support without which I could not have completed my project successfully and all these helped me to reach this stage of my life. I am grateful to them for being always understanding which makes me feel special.*

Place:
Date:

……..
Ms. Susmita Basak

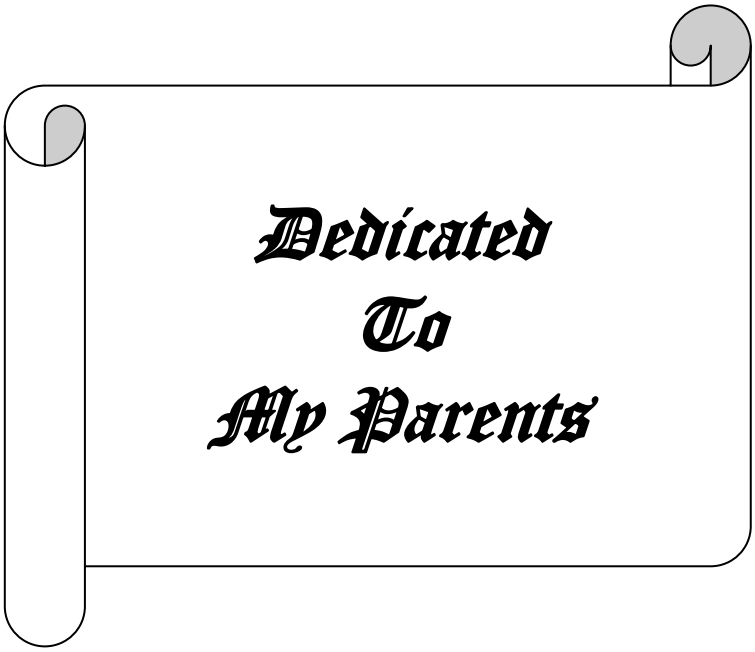
Dedicated
To
My Parents

INDEX

Figure captions

Table captions

Chapter 1

Introduction

Contents

1. Introduction

"Pharmaceutical nanotechnology" is a rising branch, which presents new tools, opportunities, and scopes in the applications of disease diagnosis and treatment (Patel et al., 2018). Now-a-days, nanotechnology research has made great roles in the area of pharmacy, especially in the drug delivery systems (Bhatia, 2016). Pharmaceutical nanoparticles are defined as sub-nanosized colloidal structures composed of synthetic or semi-synthetic polymers (with the size range of 10-1000 nm) (Pal et al., 2011). Nanotherapy is a branch of nanomedicine, which involves using nanoparticles to deliver a drug to a given target in the body for treating the disease through a process known as specific targeting (Singh et al., 2009). Compared to the conventional methods, this method has gained more popularity because it promises high precision of therapeutic achievement (Jahan et al., 2017). In the conventional therapy, there is no targeting, which means that the drug has to be transported through the circulatory system to the affected part of the body to produce its action. In this process, the drug may likely be affected by various physiological factors and/or react with other biomolecules (Jahan et al., 2017). As a result, this method has been found to possess various problems including adverse reactions, poor availability at the desire site, and concomitant elimination (Jahan et al., 2017). Assembling a nanocarrier with the nanomaterial would promote its functionalization by ensuring the longevity in circulation, site specificity, and stimuli sensitivity of the formulated nanomaterials (Lombardo et al., 2019).

1.1. Limitations of conventional chemotherapy

Conventional chemotherapeutic agents work by destroying rapid cell division, which is the main characteristic of neoplastic cells (Ricci et al., 2006). During this process, conventional chemotherapeuticals also target normal healthy cells, which are dividing rapidly, such as cells in the bone marrow, macrophages, digestive tract, and hair follicles (Ricci et al., 2006). Therefore, the main drawback of conventional chemotherapy is the lack of site specificity (Moorthi et al., 2011). This results in common side effects of most of the chemotherapeutic agents, which include myelo-suppression, mucositis, alopecia, organ dysfunction, and even anaemia or thrombocytopenia (Sutradhar et al., 2014). These side effects sometimes impose dose reduction, treatment delay, and often discontinuation of the treatment (Ricci et al., 2006). In case of solid tumors cell division may be effectively ceased near to the center, which makes chemotherapeutic agents ineffective (Shewach et al., 2009).

Furthermore, chemotherapeutic agents often cannot penetrate to reach at the core of solid tumors and fail to kill the cancerous cells (Shewach et al., 2009). In addition, traditional chemotherapeutic agents often get washed out from the circulation being engulfed by the macrophages (Shewach et al., 2009). Thus they remain in the circulation for a very short time and cannot interact with the cancerous cells making the chemotherapy completely ineffective (Shewach et al., 2009). The poor solubility of the drugs is also a major problem in conventional chemotherapy making them unable to penetrate the biological membranes (Tran et al., 2017). Another problem is associated with P-glycoprotein, a multidrug resistance protein, is over-expressed on the surface of the cancerous cells (Callaghan et al., 2014). It prevents drug accumulation inside the tumor, acting as the efflux pump, and often mediates the development of resistance to anticancer drugs (Sutradhar et al., 2014). Thus the administered drugs remain unsuccessful or cannot bring the desired output (Sutradhar et al., 2014).

1.2. Nano-chemotherapy: how it works

One of the biggest issues with conventional methods is that the drug product is distributed throughout the body and targets both healthy and cancerous cells, which in turn impede the effectiveness of chemotherapy (Hu et al., 2012). In addition, it would also impart toxic effects to the healthy cells, causing patients to present a variety of undesirable symptoms (Hu et al., 2012). It is the reason that most cancer patients tend to be hesitant while are appearing for chemotherapy (Hu et al., 2012). On the other hand, nano-carrier orchestrated nanoformulation offers to deliver the drug molecule to the affected cells in order to treat the disease without imparting negative effects to the healthy cells (Din et al., 2017). Nanotherapy acts by two ways (Ediriwickrema et al., 2015). These are passive targeting and active targeting (Ediriwickrema et al., 2015).

1.2.1. Passive targeting

Passive targeting approach is based on the enhanced permeation and retention effect (EPR) (Bazak et al., 2014). As tumorous cells continue to grow, new blood vessels are formed in order to supply the nutrients and oxygen to the new cells (Nussenbaum et al., 2010). However, these vessels are poorly formed and possess large pores that make them leaky (Nussenbaum et al., 2010). As such, they allow large molecules to pass through (Nussenbaum et al., 2010). On the other hand, these abnormal masses lack a normal lymphatic system, which impede clearance. As a result, the tumor cells retain the molecules that are allowed in (Bazak et al., 2014). Because of these

characteristics, nanoparticles that pass through into these masses are retained, which in turn allows for drug accumulation into these cells for enhanced treatment (Bazak et al., 2014). This feature is called the EPR effect and facilitates tumor interstitial drug accumulation (Figure 1.1) (Bazak et al., 2014). Due to this effect, drug loaded nanocarrier system of size below 700 nm accumulates within the tumor mass through the leaky vasculatures (Bazak et al., 2014). Nanoparticles can easily accumulate selectively through enhanced permeability and retention effect and then diffuse into the cells (Bazak et al., 2014).

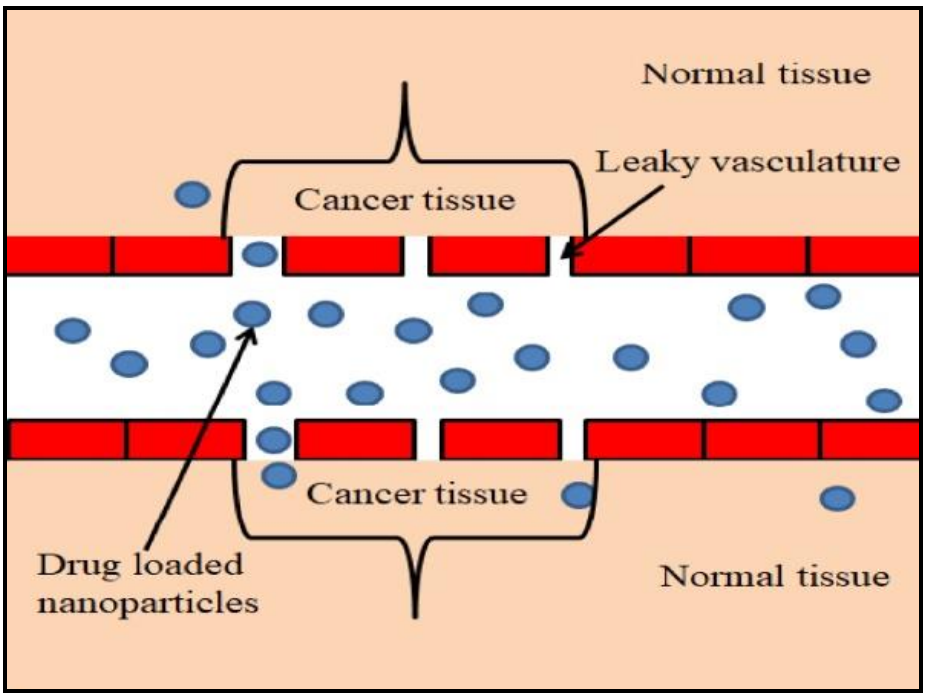

Figure 1.1. A schematic overview of passive targeting.

1.2.2. Active targeting

Active tumor targeting is used to overcome the limitations of passive accumulation (Wakaskar, 2017). Here, targeting serves to ensure the uptake of nanoparticles into the cells as well as into the intracellular compartments (Wakaskar, 2017). This is made possible by adding a number of molecules on to the surface of the nanoparticle. These include antibodies, aptamers, peptides etc (Sutradhar et al., 2014). These additional molecules on the surface of the nanoparticles are essential in active targeting given that they enhance targeting, where they serve to bind with the receptors of the target cells (Sutradhar et al., 2014). A schematic overview of active targeting has been depicted in Figure 1.2.

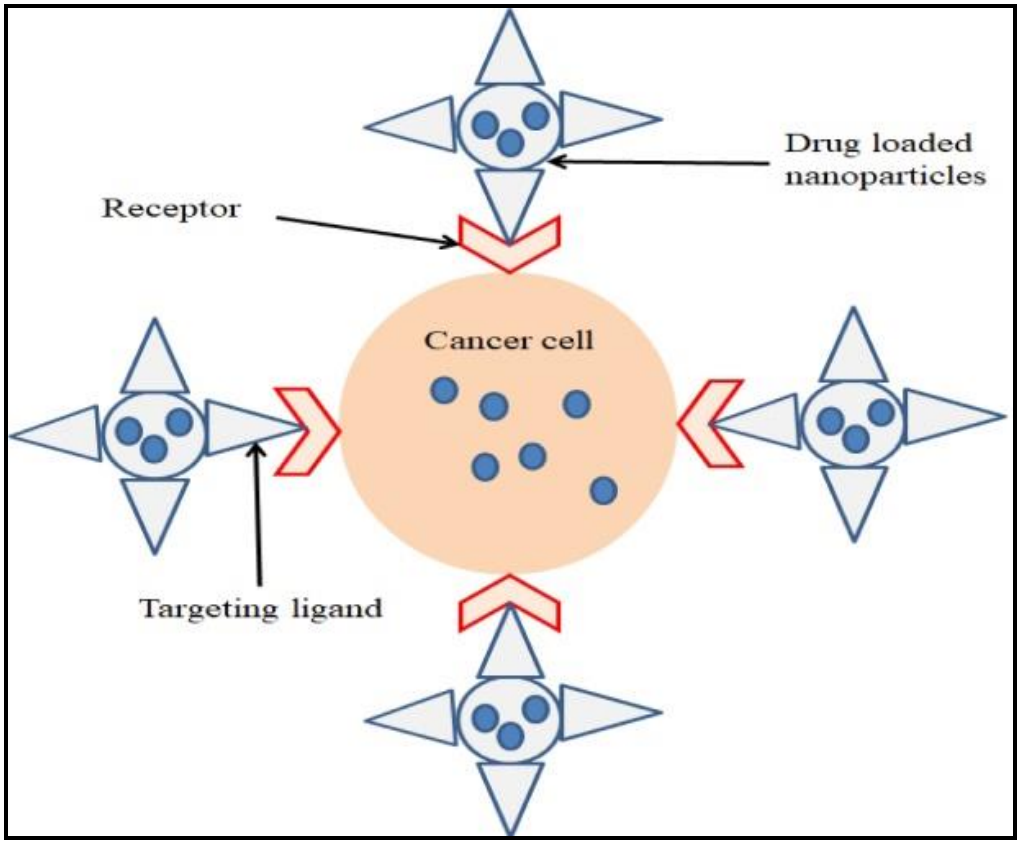

Figure 1.2. A schematic overview of active targeting.

1.3. Advantages of nanotherapy

Although nanoparticles are very small, they provide larger surface area, which presents a significant advantage in the drug delivery (Singh et al., 2009). Large surface area is a big advantage as it allows an opportunity for scientists to continually modify the molecules the way they want for different purposes (Singh et al., 2009). As such, it allows for increased functionalities of the nanoparticles (Singh et al., 2009). In addition to a large surface area, the drug release can be monitored (Singh et al., 2009). In addition, the nanoformulation offers better stability, which prevents the wastage of the drug product and ensures to deliver sufficient amounts of drug to the target cells (Rizvi et al., 2018). In cancer chemotherapy, it has been shown to be beneficial as it improves the efficiency and cost-effectiveness of the treatment (Din et al., 2017).

Since most drugs tend to be hydrophobic, these are poorly dispersed in water based biological solutions (Narvekar et al., 2014). As a result, some of the drugs are not absorbed into the vascular system resulting insufficient quantity of drug at the target cells/ tissue (Narvekar et al., 2014). With nanotherapy, this problem can be highly

minimized by modifying the surface of the nanoparticle by adding hydrophilic groups to enhance their solubility (Rizvi et al., 2018). Thereby nanotherapy enhances specificity of drug delivery by increasing the concentration of the drug molecule at the target site without affecting normal cells/ tissues (Rizvi et al., 2018).

1.4. Nano-chemotherapy: current challenges

Although nanotherapy presents many advantages in the treatment of diseases like cancer, it simultaneously faces a number of challenges that are yet to be overcome (De Jong et al., 2008). The body's defense system is one of the challenges faced in the nanotherapy (De Jong et al., 2008). Nanoparticles are often identified as foreign substances and cleared by the body through its normal homestatic mechanisms (De Jong et al., 2008), which has been shown to reduce the efficiency of nanotherapy (De Jong et al., 2008). In order to eradicate this problem, researchers are still working to develop long lasting nano-molecules or controlled nano-carriers (De Jong et al., 2008). In addition, the advantageous effective surface area of nanoparticles has simultaneously been revealed to be a major challenge in nanotherapy (Baer et al., 2013). The big surface area results in high surface energy, which encourages binding of unwanted proteins to the nano-structure (Baer et al., 2013).

Some of the proteins that bind to the surface were found to activate MPS macrophages, which in turn engulf the nanoparticles (https:// www.microscopemaster.com/nanotherapy.html, visited on April 5, 2019), which obstructs nanotherapy to be the ideal form of therapy. Researchers are trying hard to overcome this challenge (https://www.microscopemaster. com/nanotherapy.html, visited on April 5, 2019).

1.5. Types of nanoparticles

Depending on the applications, such as diagnosis, imaging, and therapy, nanoparticles types are divided in two main groups, namely organic and inorganic nanoparticles (Parveen et al., 2012). The first group includes micelles, dendrimers, liposomes, and compact polymeric nanoparticles (Figure 1.3), while the second group includes fullerenes, quantum dots, silica and gold nanoparticles (Rangasamy, 2011).

1.5.1. Organic nanoparticles

1.5.1.1. Dendrimers

Dendrimers are nano-sized, radially symmetrical structures with well-defined, homogeneous, and monodisperse structure (Roeven et al., 2019). These are morphologically characterized by branched structures grown from one or more cores

(Roeven et al., 2019). The size of these nanoparticles can be easily controlled by monitoring the number of generations (Roeven et al., 2019). However, dendrimers present difficulties regarding drug incorporation and release as their syntheses are quite time-consuming.

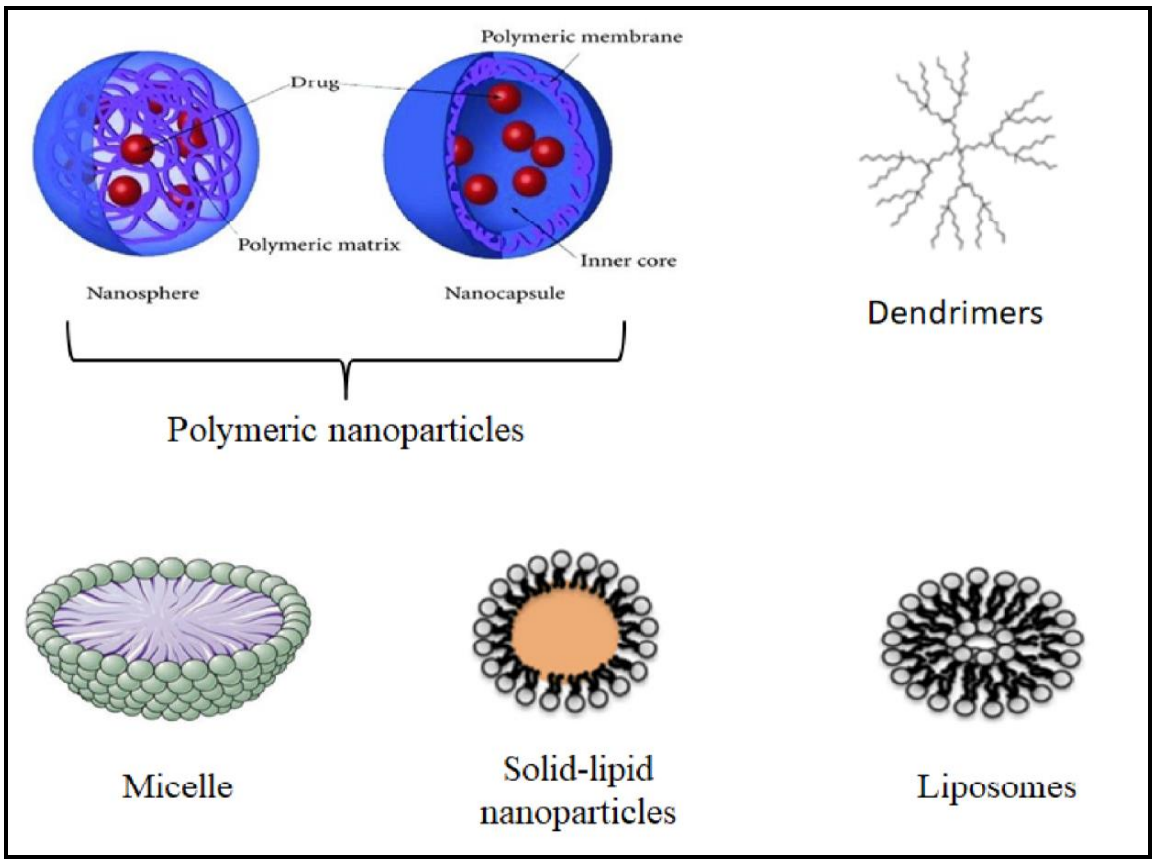

Figure 1.3. Different types of nanoparticles.

1.5.1.2. Micelles

Micelles are nanostructures made of amphiphilic molecules, like polymers or lipids (Orive et al., 2009). When exposed to aqueous environments, they hide their hydrophobic groups inside the structure and expose the hydrophilic groups (Orive et al., 2009). On the other hand, these may organize the structure in a reverse way in the lipid-enriched environment (Orive et al., 2009). Poorly water-soluble drugs can be loaded into the micelles hydrophobic core, while amphiphilic drugs align with the micelle amphiphilic structure keeping the polar groups near to the hydrophilic groups of the micelle (Bamrungsap et al., 2012). Micelles are stable due to their hydrophilic shell and have prolonged circulation time in the blood (Bamrungsap et al., 2012).

1.5.1.3. Liposomes

Liposomes are vesicles made entirely of lipidic compounds (Ratner et al., 2014). The most common are the unilamellar liposomes with the particle size ranging between 100 and 800 nm (Akbarzadeh et al., 2013). These spherical structures with amphiphilic compounds present high production cost and content leakage (Akbarzadeh et al., 2013). As the main advantages, these are completely biodegradable, compatible, non-toxic, and non- immunogenic (Akbarzadeh et al., 2013).

1.5.1.4. Polymeric nanoparticles

Polymeric nanoparticles are nanostructures made entirely of natural or synthetic polymers (Orive et al., 2009). These are usually more stable than liposomes allowing sustained localized drug delivery for weeks with reduced drug leakage (Orive et al., 2009). In these polymeric nanostructures, the therapeutic agent can be eventually linked covalently (Reis et al., 2006). Alternatively, therapeutic agents can be adsorbed at the surface of nanoparticles or dissolved in or entrapped within the structure of nanoparticles structure (nanospheres) or encapsulated inside a polymeric shell (nanocapsules) (Pal et al., 2011; Reis et al., 2006). Polymers which are used for nanoparticles formulation are either natural or synthetic. Natural polymers used in polymeric nanoparticles include proteins, such as gelatin, albumin, lectins, legumin etc. and polysaccharides, such as alginate, dextran, chitosan, agarose etc (Jain, 2001). On the other hand several synthetic polymers, such as polylactides (PLA), polyglycolides (PGA), poly(lactide co-glycolides) (PLGA), polyanhydrides, polyorthoesters, polycyanoacrylates, polycaprolactone, poly glutamic acid, polymalic acid, poly(N-vinyl pyrrolidone), poly(methyl methacrylate), poly(vinyl alcohol), poly(acrylic acid), poly acrylamide, poly(ethylene glycol), poly(methacrylic acid) etc. are used in developing polymeric nanoparticles (Jain, 2001).

1.5.2. Inorganic nanoparticles

1.5.2.1. Quantum dots

Quantum dots are nanometric and multifunctional inorganic fluorophores, which are used in imaging, detection, and targeting (Ghasemi et al., 2009; Slotkin et al., 2009; Michalet et al., 2005). These are generally luminescent semiconductor crystals (Ghasemi et al., 2009; Slotkin et al., 2009; Michalet et al., 2005). Quantum dots are made of elements from groups II-VI or III-V, being their structure generally based on cadmium sulfide (CdS) and cadmium selenide (CdSe), which can be highly toxic

(Ghasemi et al.,2009; Fernandez-Fernandez et al., 2012). As advantages, comparing to traditional fluorophores (organic dyes and fluorescent proteins), quantum dots present a broad absorption range and narrow emission spectra (Gao et al., 2004). In fact, these possess tunable size emission with different wavelengths over a broad range of the light spectrum (Gao et al., 2004). Additionally, quantum dots present high photostability (Bailey et al., 2003) being remarkably resistant to photobleaching (Dubertret et al., 2002). The use of quantum dots is based on their unique chemical and physical properties, which are achieved due to their size and highly compact structure (Ghasemi et al., 2009).

1.5.2.2. Fullerenes

Fullerenes are allotrope of carbon. Fullerenes nanoparticles are simply made of carbon molecules of highly symmetric and stable forms (Chen et al., 2012). Buckminsterfullerene (C60), the most well-known fullerene, is a rigid icosahedron with 60 carbon atoms. In its structure, single bounds form pentagons and double bounds form hexagons (Ma et al., 2010). Fullerenes disadvantages, such as the low solubility in organic solvents can be overcome by their unique optic, electric and magnetic properties (such as super-conductivity 80), which render them the important devices in medical diagnosis and imaging (Bosi et al., 2003).

1.5.2.3. Silica and gold nanoparticles

Inorganic materials, such as gold, silver, platinum, and silica can also be used to produce nanoparticles (Kim et al., 2014). Inorganic nanoparticles can be prepared by different methods, forming a highly ordered and rigid three-dimensional arrangement with metal or covalently linked atoms (Kim et al., 2014). Their properties, such as size and shape, are almost not influenced by the in vivo conditions, unlike organic nanoparticles (Kim et al., 2014). However, the drawbacks of inorganic nanoparticles have to be taken into account (Mishra et al., 2013). In the case of metallic nanoparticles, it is very challenging task to load the drugs into their structure (De Jong et al., 2008; Mishra et al., 2013). In addition, negative effects of metallic nanoparticles to the blood have to be considered (De Jong et al., 2008; Mishra et al., 2013). However, their high potential as magnetic responsive nanoentities is of great importance and has been extensively reviewed in the literature (Santo et al., 2013). On the other hand, silica nanoparticles have been associated with cytotoxic effect related to an increase in the level of reactive oxygen species and decrease in glutathione level (Lin et al., 2006).

1.6. State of art and objective

Asiatic acid, (2, 3, 23-trihydroxy-urs-12-ene-28-oic-acid), is a naturally occurring aglycone of pentacyclic triterpene (Lv et al., 2018). Asiatic acid is commonly present in the leaves of *Centella asiatica* Urban. (Lv et al., 2018). It has been reported to possess antioxidant (Lv et al., 2017), anticancer (Hsu et al., 2005), and anti-inflammatory (Lv et al., 2017), and antidiabetic (Sun et al., 2017) activities. But, asiatic acid has poor bioavailability as it undergoes rapid metabolism (Meeran et al., 2018). Therefore, it has been aimed to improve the bioavailability of asiatic acid through formulating asiatic acid-loaded polymeric nanoparticles. The present research deals with formulation and characterization of PLGA polymer-based asiatic acid nanoparticles.

The salient features to achieve the objectives were

i. To formulate PLGA-based asiatic acid nanoparticles using multiple emulsions and solvent evaporation method

ii. To perform characterization of the developed nanoparticles through particle size analysis, surface morphology assessment, drug distribution study, drug-excipients incompatibility assessment, and in vitro drug release studies.

Chapter 2

Literature review

Contents

2. Literature review

2.1. Asiatic acid

Asiatic acid (figure 2.1) is a naturally occurring aglycone of pentacyclic triterpene isolated from the dried leaves of *Centella asiatica* Urban. belonging to the family Apiaceae (Meeran et al., 2018). It is a naturally occurring bioactive lead against various ailments (Meeran et al., 2018).

2.2. Details of asiatic acid

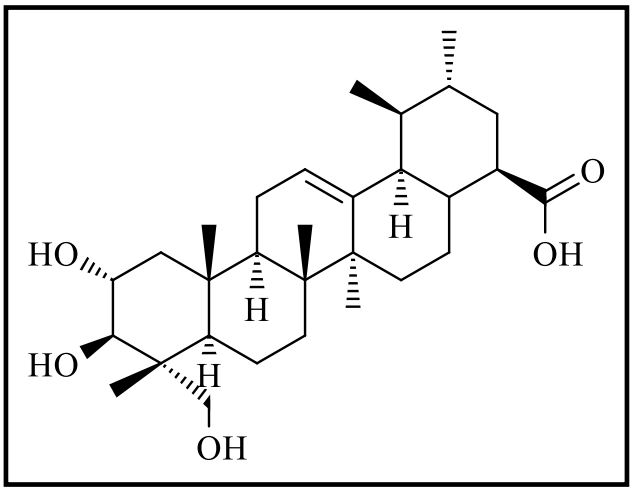

Figure 1.1. Chemical structure of asiatic acid.

Chemical formula: $C_{30}H_{48}O_5$ (Lv et al., 2018).

Molar mass: 488.7 g/mol (Lv et al., 2018).

Melting point: 325- 330 °C (Lv et al., 2018).

Appearance: White powder (Lv et al., 2018).

Storage: For long term storage, asiatic acid should be stored at -20°C. It should be stable for at least for two years (Lv et al., 2018).

Solubility: Asiatic acid is soluble in organic solvents such as ethanol, DMSO, and dimethyl formamide (DMF), which should be purged with an inert gas (Zhao et al., 2010). The solubility of asiatic acid in ethanol is approximately 10 mg/ml and approximately 20 mg/ml in DMSO and DMF (Zhao et al., 2010). Asiatic acid is sparingly soluble in aqueous buffers (Zhao et al., 2010). For maximum solubility in aqueous buffers, asiatic acid should first be dissolved in DMSO and then diluted with the aqueous buffer of choice (Zhao et al., 2010).

2.3. Pharmacological effects of asiatic acid

2.3.1. Antioxidant activity of asiatic acid

Asiatic acid has been found to exhibit potent antioxidant and free radical

scavenging properties involving various pathways (Liu et al., 2018). It could produce concentration-dependent free radical scavenging activity by countering hydroxyl radicals and superoxide anions (Liu et al., 2018). The antioxidant-mediated protective effects of asiatic acid have been demonstrated in various experimental models (Lv et al., 2017). Asiatic acid is a highly effective chain-breaking antioxidant, which can act against reactive oxygen species (ROS) (Lv et al., 2017). It has been reported to attenuate myeloperoxidase activation and inhibit lipid peroxidation (Lv et al., 2017). The inhibitory capacity on lipid peroxidation has been found to be higher than several well-known antioxidants, such as probucol, ascorbic acid, and α- tocopherol (Ramachandran et al., 2013). It was also found to augment activities/levels of both enzymatic and non-enzymatic antioxidants (Ramachandran et al., 2013).

2.3.2. Anti-Inflammatory activity of asiatic acid

Asiatic acid has been found to possess anti-inflammatory activity and to prevent the development and progression of immune-inflammatory disorders via inhibition of pro-inflammatory cytokines (Chen et al., 2017). The NF-κB inhibitory activity of asiatic acid has been supported by the in silico and in vitro studies (Patil et al., 2015; Kamble et al., 2017). Asiatic acid could ameliorate NF-κB expression in LPS-stimulated RAW264.7 cells, inhibited IKKα/β phosphorylation and interferon-gamma (IFN-γ) activation (Patil et al., 2015; Kamble et al., 2017). In silico molecular docking studies predicted of NF-κB inhibitory activity of asiatic acid (Patil et al., 2015; Kamble et al., 2017). Asiatic acid exhibited anti-complement activity as evidenced by the inhibition of the hemolytic activity of human serum against erythrocytes in micromolar concentrations (Patil et al., 2015; Kamble et al., 2017). This activity is attributed by the carboxylic group present in the structure of ursane type triterpenoids (Patil et al., 2015). Asiatic acid was found to inhibit pathways initiated by the activation of toll-like receptors, which lead to the expression of pro-inflammatory cytokines (IL-1β, IL-6, IL-8, and TNF-α) (Chen et al., 2017). In a fluorescent based assay, asiatic acid impaired endothelial cell activation on monocyte adhesion and migration (Fong et al., 2016). The endothelial cell activation plays an important role in the atherogenesis and other chronic inflammatory diseases (Fong et al., 2016). Asiatic acid was shown to inhibit endothelial hyperpermeability, enhanced VCAM-1 expression and improve

the levels of soluble CAMs (sE-selectin, sICAM-1, sVCAM-1, and sPECAM-1) provoked by TNF α (Fong et al., 2016). Asiatic acid has been found to attenuate TNF-α-triggered phosphorylation of IkB- α (Fong et al., 2016).

2.3.3. Anti-diabetic activity of asiatic acid

Asiatic acid was found to exhibit weak α-amylase and α-glycosidase inhibitory activities (Hou et al., 2009). It was found to exert anti-hyperglycaemic effect by preserving the damage of β-cells of pancreas and restoring their functions in rodent models of diabetes (Liu et al., 2010). Thereby, asiatic acid could enhance serum insulin level produced by the pancreatic β cells in diabetic rats (Liu et al., 2010). Mechanistically, it promoted cell survival machinery by promoting activation of Akt kinase and Bcl-xL in the pancreatic islets (Sun et al., 2017). The antidiabetic activity of asiatic acid has been shown to be mediated by PI3K/AKT/GSK-3β signaling mechanism in high-fat diet fed db/db mice (Sun et al., 2017). The observed antidiabetic effect has been evidenced by the normalization of blood glucose and lipid levels and glycogen synthesis along with histological salvage (Sun et al., 2017). Ramachandran and Saravanan (2013) have demonstrated that oral administration of asiatic acid to diabetic rats decreased the levels of blood glucose, increased insulin levels and corrected glycosylated haemoglobins. It could also decrease the activities of glucose-6-phosphatase and fructose-1,6-bisphosphatase and increased the activities of hexokinase, pyruvate kinase, glucose-6-phosphate dehydrogenase involved in carbohydrate metabolism (Ramachandran et al., 2015). Additionally, it could increase the level of liver glycogen and normalize the activities of liver markers enzymes in diabetic rats (Ramachandran et al., 2015). The anti-hyperglycemic effect of asiatic acid has been found to be equivalent to glibenclamide, a standard anti-hyperglycaemic drug (Ramachandran et al., 2015). Furthermore, asiatic acid normalized the levels of blood glucose, improved insulin levels, restored antioxidant defense system, and reduced lipid peroxidation. In the molecular level, asiatic acid was found to activate promote glucose utilization by activating IRS-1/2/PI3K/Akt signaling followed by the translocation of glucose transporter 4 (GLUT4) proteins to the membrane (Ramachandran et al., 2015). In molecular docking, asiatic acid showed affinity against HMG-CoA reductase, an enzyme involved in cholesterol biosynthesis with a binding energy Wang et al. (2015) have demonstrated that asiatic acid prevented islets dysfunction and lowered blood glucose levels in Goto

Kakizaki rats (Wang et al., 2015). Asiatic acid (0.1 or 0.2%) was found to protect the diabetic heart by reducing localized injury and coagulation components (Hung et al., 2015). It could reduce the levels of plasma glucose, creatine phosphokinase, lactate dehydrogenase, and restored HbA1c levels in diabetic mice. It has been found to reduce ROS, N (+)-(carboxymethyl)-lysine, pentosidine, methylglyoxal, pro-inflammatory cytokines, and chemokines levels in diabetic mice. Asiatic acid could also decrease the activities of NADPH oxidase and aldose reductase (Wen et al., 2008). It was found to impede the expressions of glyoxalase 1, NF-κB, phosphorylated p38, phosphorylated ERK1/2, and the receptors of advanced glycation products in diabetic heart (Wen et al., 2008).

2.3.4. Asiatic acid in cardiac hypertrophy

The effects of asiatic acid on cardiac hypertrophy and underlying mechanism were studied using pressure overload-induced mouse model of cardiac hypertrophy and cultured neonatal cardiomyocytes stimulated with TGF-β1 (Si et al., 2014). Asiatic acid has been found to attenuate cardiomyocyte hypertrophy by reducing the surface area and by inhibiting the expressions of atrial natriuretic peptide, phosphorylated p38, phosphorylated ERK1/2, and NF-κB (Si et al., 2014). Asiatic acid could also reduce the activation TGF-β1 signaling in the pressure-overload mice model of cardiac hypertrophy (Si et al., 2014). In another study by Xu et al. (2015), asiatic acid was found to reinstate transverse aortic constriction-induced cardiac hypertrophy in C57BL/6 mice and cultured neonatal cardiomyocytes (Xu et al., 2015). AA was found to inhibit IL-1β-triggered hypertrophic signaling that suppressed cardiac hypertrophy (Xu et al., 2015). Similar observation has been noted in another study in a transverse aortic constriction mice model mimicking the progression of hypertrophy and heart failure (Si et al., 2015), in which asiatic acid attenuated intrinsic and extrinsic apoptotic signaling, interstitial fibrosis, and inflammation by blocking the activation of both transforming growth factor-β1/Smad and IL-6 (Si et al., 2015). Further, it appears to be protective against coronary artery ligation-induced myocardial ischemia in rats (Si et al., 2015). Asiatic acid treatment has been shown to improve cardiac functions, reduced inflammatory cytokines and interstitial fibrosis (Si et al., 2015). Asiatic acid also prevented the left ventricular remodeling of the ischemic myocardium by inhibiting phosphorylation of p38 and ERK1/2 (Si et al., 2015). Kalyanavenkataraman et al. (2016) proposed another cardio-protective mechanism

wherein it appears to bathe most potent agent in inhibiting carbonic anhydrase II with an IC_{50} of 9 μM (Kalyanavenkataraman et al., 2016). In addition, it was found to inhibit cytosolic activity in H9c2 cardiomyocytes accompanied by decreased intracellular levels of Ca^{+2}, acidification, and mitochondrial membrane depolarization (Kalyanavenkataraman et al., 2016). In another study, asiatic acid attenuated doxorubicin-induced oxidative stress and inflammation in the heart, liver, and kidney by up-regulating nuclear factor erythroid 2-related factor 2 (Nrf2) protein expression (Kamble et al., 2018). Recently, asiatic acid was shown to inhibit pressure overloaded or angiotensin II-induced hypertrophic responses by suppressing collagen accumulation. Mechanistically, the protective effects of asiatic acid have been found to be mediated through the activation of 5' AMP-activated protein kinase (AMPK) and inhibition of the mammalian target of rapamycin (mTOR) pathway (Meeran et al., 2018).

2.3.5. Asiatic acid in non-small cell lung cancer

Asistic acid has been found to exhibit therapeutic effect against non- small cell lung cancer by reducing the cell proliferation by impeding Ras/Raf/MEK/ERK pathway and arresting cell cycle at G1/S and G2/M (Wang et al., 2013). Ras/Raf/MEK/ERK signaling pathway is known to play key roles in facilitating the proliferative signal transmission from membrane-bound receptors and relay extracellular information through an interaction with various cellular proteins within the nucleus to control gene expression (Steelman et al., 2011). Asiatic acid was reported to elicit cytotoxicity mediated by microRNA (miR)-1290 , which regulates apoptotic cell death, cell viability, and cell cycle progression in A549 cells (Kim et al., 2014). It could also induce apoptosis, loss of mitochondrial membrane potential, and free radical generation along with improved microtubule associated protein 1 light chain 3 (LC3) and reduced expression of p62 (Wu et al., 2015). Orally administered asiatic acid was found to reduce the tumor volume and expression of proliferating cell nuclear antigen by promoting apoptosis in the mouse lung cancer xenograft model (Wu et al., 2015).

2.3.6. Asiatic acid in melanoma

Melanoma is the deadliest form of skin cancers and about 10%cases occur in a familial context involving cyclin-dependent kinase inhibitor 2A (CDKN2A) as a main high-risk gene for melanoma (Potrony et al., 2015). Park and co-workers (2005) have demonstrated the time- and dose-dependent anticancer activity of asiatic acid in human melanoma cells (SK-MEL-2) by inducing apoptosis and decreasing cell

viability (Park et al., 2005). Asiatic acid was found to increase the levels of ROS, Bax, and caspase-3 expressions in a concentration-dependent manner; however, it failed to raise p53 levels in the c SK-MEL-2 cells (Park et al., 2005). In another study, the antiproliferative activity of asiatic acid has been demonstrated in murine melanoma cells; B16F10 (Yoshida et al., 2005). Taken together, Asiatic acid appears as a promising agent for human skin cancer.

2.3.7. Asiatic acid in breast cancer

Asiatic acid has been found to inhibit the cell growth, to reduce cell survival, to cause cell cycle arrest in SG2/M phase, and to induce apoptosis to MCF-7and MDA-MB-231 cells; by activating of p38 and ERK1/2 signalings (Hsu et al., 2005). Asiatic acid was also found to accelerate the interaction between p21 and Cdc2 and impaired the expressions of Cdc2, Cdc25C, cyclinB1, and cyclin A. Thereby, it could inhibit cell cycle progression (Hsu et al., 2005). Therefore, asiatic acid would be a promising for chemo-preventive agent against breast cancer.

2.3.8. Asiatic acid in prostate cancer

Prostate cancer relies on androgen-dependent signalling for initiation, progression and development. In PPC-1 prostate cancer cells, asiatic acid was found to induce caspase-dependent and independent apoptotic cell death to PPC-1 prostate cancer cells (Gurfinkel et al., 2006). Asiatic acid treatment was found to disrupt endoplasmic reticulum and to alter calcium homeostasis (Gurfinkel et al., 2006).

2.4. Polylactide-co-glycolic acid (PLGA)

PLGA is one of the most effective polymers of lactide acid and glycolic acid (Figure 2.2) used in nanoformulation (Mirakabad et al., 2014). It has been approved by the US-FDA to

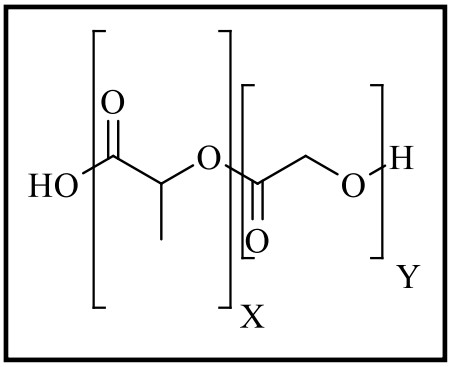

Figure 2.2. Chemical structure of PLGA.

[X = number of units of lactic acid; Y= numbers of units of glycolic acid]

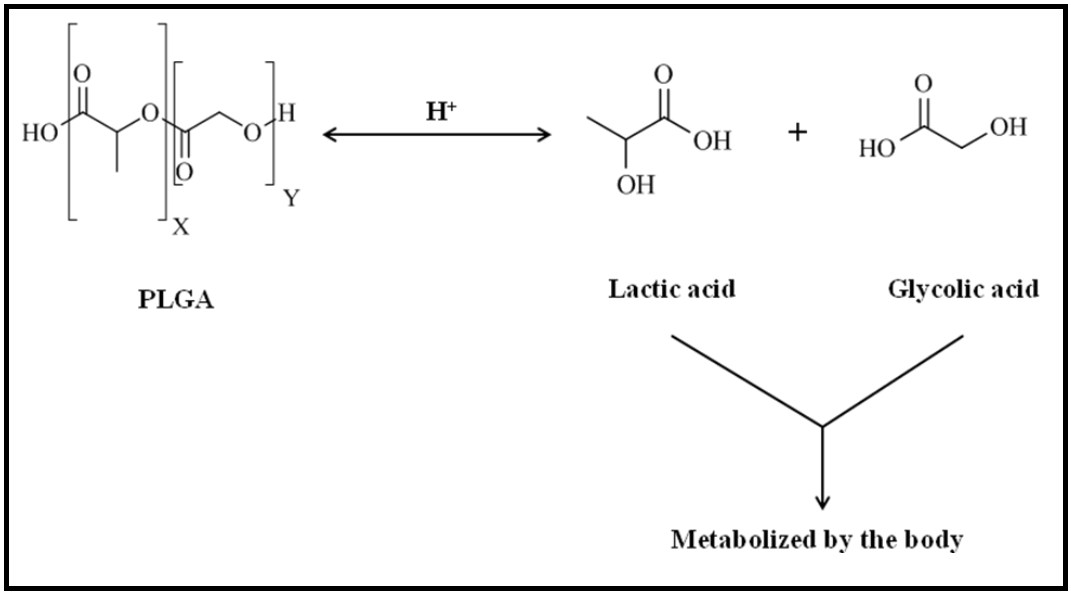

Figure 2.3. Hydrolysis of PLGA.

use in drug delivery systems due to its controlled and sustained release properties, low toxicity, and biocompatibility with the tissues and cells (Mirakabad et al., 2014). PLGA is one of the most successfully used biodegradable polymers because its hydrolysis leads to the monomers, such as lactic acid and glycolic acid (Figure 2.3). As these two monomers are endogenous and simply metabolized by the body via the Krebs cycle, a negligible systemic toxicity is associated with the use of PLGA in the drug delivery or biomaterial applications (Kumari et al., 2010; Danhier et al., 2012). Additionally, PLGA-based nanoparticles are currently under examinations for applications in cancer imaging and cancer therapy (Matsumura and Maeda, 1986; Danhier et al., 2012). Presence of more lactides and less glycolides in PLGA (85:15) showed slower release because of its high molecular weight and less hydrophilicity as compared to the other varieties of PLGA, such as PLGA such as PLGA (75:25), PLGA (65:35), and PLGA (50:50). Lactic acid is more hydrophobic than glycolic acid and, thus, lactide-rich PLGA copolymers are less hydrophilic, absorb less water, and consequently, degrade more gradually (Park, 1994; Schliecker et al., 2003; Dinarvand et al., 2011). In general, the degradation time will be shorter for low molecular weight, more hydrophilic, and more amorphous polymers as found in the copolymers with a higher glycolide content (Dinarvand et al., 2011).

2.5. Poly vinyl alcohol (PVA)

Poly (vinyl alcohol) (PVA) was first prepared by Hermann and Haehnel in 1924 by hydrolyzing polyvinyl acetate in ethanol with potassium hydroxide (Nagarkar et al., 2019). Polyvinyl alcohol is produced commercially from polyvinyl acetate, usually by

a continuous process (Nagarkar et al., 2019). The acetate groups are hydrolyzed by ester interchange with methanol in the presence of anhydrous sodium methylate or aqueous sodium hydroxide (Figure 2.4).

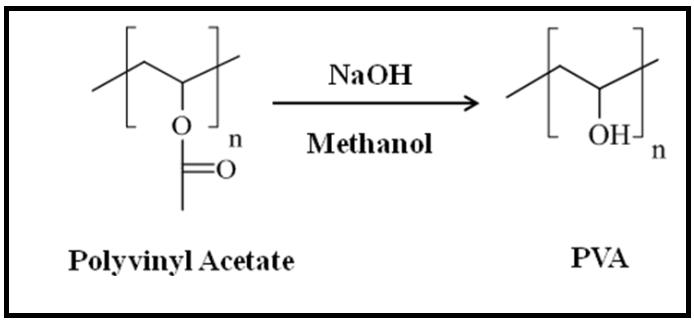

Figure 2.4. Formation of PVA.

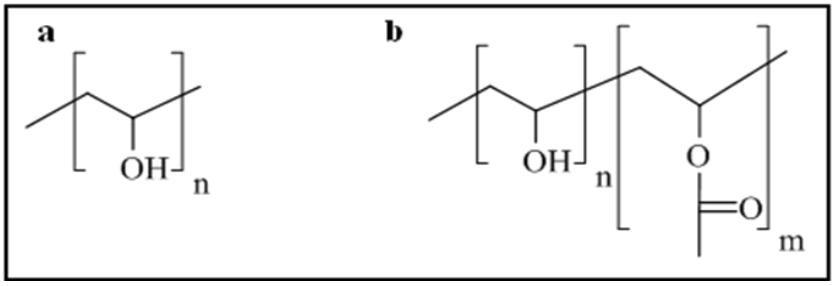

Figure 2.5. Fully hydrolysed (a) and partially hydrolysed (b) PVA.

The physical characteristics and its specific functional uses depend on the degree of polymerization and the degree of hydrolysis (Nagarkar et al., 2019). PVA is classified into two classes namely: fully hydrolyzed (Figure 2.5.a) and partially hydrolyzed (Figure 2.5.b) (Nagarkar et al., 2019). Partially hydrolyzed PVA is used in the foods (Nagarkar et al., 2019). Generally, PVA is odorless, tasteless, translucent, and white (colourless) to cream coloured granules (Nagarkar et al., 2019). It is used as a moisture barrier film for food supplement tablets and for foods that contain inclusions or dry food with inclusions that need to be protected from moisture uptake. PVA is not known to occur as naturally and it is an artificial polymer (Gaaz et al., 2015).

PVA is soluble in water, slightly soluble in ethanol, but insoluble in non-polar organic solvents (Nagarkar et al., 2019). Typically a 5% solution of PVA exhibits a pH in the range of 5.0- 6.5. PVA has a melting point of 180 to 190°C. PVA is a water soluble synthetic polymer (Nagarkar et al., 2019). It has the idealized formula $[CH_2CH(OH)]_n$ (Gaaz et al., 2015). It is sometimes supplied as beads or as solution in water (Gaaz et al., 2015). PVA, which is essentially made from polyvinyl acetate through hydrolysis,

is easily degradable by biological organisms (Gaaz et al., 2015). It is a crystalline structured polymer (Gaaz et al., 2015).

The molecular weights obtained for PVA products may vary between 20,000 and 200,000 depending on the length of the initial vinyl acetate polymer, the level of hydrolysis to eliminate the acetate groups and whether it occurs under alkaline or acidic conditions. The extent of hydrolysis can vary from a typical value of 80% to > 99% (Nagarkar et al., 2019). Nearly fully hydrolyzed forms result in forming PVA hydrogels with tuneable properties through crosslinking of the linear polymers, which subsequently result in polymer (gel)-fluid (sol) species (Gaaz et al., 2015). Polymer contents affect the physical status of the resulting material: low polymer content results in soft materials because the fluid moves freely through the matrix, whereas a higher polymer content results in considerable stiffening and strengthening of the material's matrix (Gaaz et al., 2015). Studies on the diffusive permeability of solutes in PVA gel membranes and the application for separation have been delineated because of chemical stability, particularly on film-forming, and hydrophobicity (Gaaz et al., 2015).

Chapter 3

Materials and methods

Contents

3.1. Materials and equipments

The chemicals and solvents used in this study were of analytical grade and obtained from reputed suppliers (Table 3.1.). The list of equipments used in this study has been detailed in Table 3.2.

Table 3.1. Chemicals and solvents used in formulation and their respective sources.

Chemicals and solvents	Sources
Asiatic acid (AA) 97% Sigma-Aldrich	Pharmachem & Co., Kolkata
Poly vinyl alcohol (PVA) (MW 125,000)	S.D. Fine Chem. Pvt. Ltd. Mumbai, India
Poly-lactide-co-glycolide (PLGA, 85:15)	Gifted by Prof. Parames C. Sil
Absolute ethanol	Merck Specialities Pvt. Ltd., Mumbai, India
Dichloromethane (DCM)	Merck Specialities Pvt. Ltd., Mumbai, India
Acetone	Merck Specialities Pvt. Ltd., Mumbai, India
Dimethyl sulfoxide (DMSO, analytical grade)	Fisher Scientific, UK. CBQCA
Milli-Q Water	Department of Pharmaceutical Technology, Jadavpur University, Kolkata

Table 3.2. Equipments used in this study.

Equipments	Details
Electronic balance	Satorius, Gőttingen, Germany
High speed homogenizer	Model T10B, Ultras-Turrax, IKA Laboratory Equipment, Staufen, Germany
Cold centrifuge	3k30, Sigma, Allentown, USA
Lyophilizer	Laboratory Freeze Dryer, Instrumentation India Ltd., Kolkata, India
Magnetic stirrer	Remi Equipments, Mumbai, India
UV-vis-spectrophotometer	Varian, Palo Alto, USA
Eco ATR	Model- Alpha, Bruker, Germany
Field emission scanning electron microscope	Model-HITACHI S-4800, JEOL, Tokyo, Japan
Zetapotential and particle size analyzer	Model- Zetasizer Nano ZS90, Malvern Instruments, Malvern, UK
Transmission electron microscope	Model: JEOL 2100, Operating Voltage: 200 KV,

	Resolution : 0.19 nm, FEI, Praha, Czech Republic
Ultrasonic water bath	Trans-o-sonic, Mumbai, India
CO_2 incubator	Model MCO-15AC, Sanyo Electric Biomedical Co. Ltd., Osaka, Japan
Vortex mixer	Remi, Mumbai, India
Atomic Force microscopy	Model-Solver Pro, Bruker, Karlsruhe, Germany
Nuclear magnetic resonance (NMR) spectrometer	Bruker DRX 300 MHz spectrometer, UK

3.2. Methodology

3.2.1. Preparation of nanoparticles

Asiatic acid nanoparticles were prepared by multiple emulsion solvent evaporation technique. In the first step, the aqueous PVA solutions of 1.5% (w/v) and 2.5% (w/v) were prepared by dissolving the PVA in warm water (Paul et al., 2018). Then, in the second step, approximately 50 mg of PLGA was solubilized in 3 ml of organic phase containing DCM and acetone (4:1, w/w ratio) and the beaker containing this mixture was kept on the magnetic stirrer. After 5 minutes, the mixture of asiatic acid and DMSO was added to the beaker, which was kept on the magnetic stirrer. After that, the beaker was covered with aluminium foil and it was left for 15 minutes. In the third step, the organic polymeric solution containing asiatic acid was emulsified quickly with drop wise gradual addition of 2.5% (w/v) PVA solution, and continuous homogenization for 5 min using a high-speed homogenizer at 20,000 rpm (IKA Laboratory Equipment, Model T10B, Ultra-Turrax, Staufen, Germany). Thus the primary emulsion was formed. This primary emulsion was quickly added to 75 ml of 1.5% PVA solution and homogenized for about 8 min at 20,000 rpm to get secondary emulsion (Paul et al., 2018). In the fourth step, the emulsion thus obtained was kept in a bath sonicator for 10-15 min to break the large globules and then stirred on a magnetic stirrer overnight without heating for complete removal of organic solvents used to dissolve the polymer (Paul et al., 2018). The organic phase was allowed to diffuse out and evaporated to get homogenous nanoparticles. While nanoparticles were hardening, the particles suspension was kept on a bath sonicator (Trans- O-sonic, Mumbai, India) for about 45 min to break the agglomerates, if any. In the fifth step, the nanoparticles were then first separated by centrifugation at 5000 rpm for 10 min to separate larger particles and then the supernatant was collected and re-centrifuged at 16,000 rpm for 30 min (Paul et al., 2018). The solid particles were re-

suspended in Milli-Q water, and centrifuged to wash out the excess PVA attached on surface of the nanoparticles and the free drug (Lamprecht et al. 1999). The washing was repeated for three times. In the sixth step, the separated nanoparticles were then kept in petridish in an ultrafreezer (So Low, Environmental Equipment, OH, USA). After that, the frozen sample was lyophilized in a freeze dryer (Laboratory Freeze Dryer, Instrumentation India, Kolkata, India) for 7-8 h to obtain a solid product (Paul et al., 2018).

3.2.2. Drug-excipients interactions

3.2.2.1 Attenuated total reflection (ATR) spectroscopy

Eco ATR (Model-Alpha; Bruker, Germany) was used to obtain ATR spectra of asiatic acid, PLGA, PVA, their lyophilized mixtures and the prepared nanoparticles. The absorption spectra in the infrared region for the samples were within the range of 4000 cm^{-1} to 600 cm^{-1}. The spectra were obtained at room temperature (± 20˚C) with the sample added directly into the device, with no prior treatment.

3.2.2.2. Nuclear magnetic resonance (NMR) spectroscopy

NMR spectroscopy (Bruker DRX 300 MHz spectrometer) was used to obtain NMR spectra of AA, PLGA and their physical mixture. $CDCl_3$ solvent was added with each of these samples in the NMR tube and vortexed to dissolve them very well (https://www.cif.iastate.edu/nmr/nmr-tutorials/sample-preparation, viewed on May 10, 2019).

3.2.3. Physico-chemical characterization of nanoparticles

3.2.3.1. Determination of drug loading and drug entrapment efficiency

For determination of drug loading, accurately weighed amount of (1.2 mg) Asiatic acid nanoparticles was taken into a centrifuge tube and 1.2 ml of ethanol was added and then vortex and then sonicated for 15 min (Paul et al., 2018). After that it is kept for 2-3 h at 37 °C in room temperature (Paul et al., 2018). Then it is centrifuged at 16000 rpm for 10 min (Paul et al., 2018). Then the supernatant was collected and released drug was assayed spectrophotometrically at 210 nm.

Percentage of actual drug loading was calculated from equation (1) (Paul et al., 2018).

Actual drug loading = Amount of drug present in nanoparticles / Weight of nanoparticles sample analysed x 100 .....(1)

Percentage of theoretical drug loading was calculated from equation (2) (Paul et al., 2018).

Theoritical drug loading = Amount of drug / (Amount of drug + Amount of polymer) x 100 .....(2)

Drug entrapment efficiency was calculated from equation (3) (Paul et al., 2018).

Drug entrapment efficiency = Drug loading (actual) (%) / Drug loading (theoretical) (%) x 100.....(3)

3.2.3.2. Particle size distribution & zeta potential measurement

The average particle size and zeta potential values of all the experimental formulations were measured using Malvern Zetasizer Nano-ZS90 (Malvern Instruments, Malvern, UK) utilizing dynamic light scattering (DLS) technique (Satapathy et al., 2016). A weighed quantity of the experimental sample was dispersed in Milli-Q water (Millipore Corp., MA, USA) followed by sonication and vortexing before placing it in the cuvette for the measurements of particle size and zeta potential (Das et al., 2015; Maji et al., 2014).

3.2.3.3. Particle size measurement using field emission scanning electron microscopy (FE-SEM)

Particle morphology was assessed by field emission scanning electron microscope (FESEM; Model-HITACHI S-4800). The lyophilized particles were placed on a carbon tabs mounted on SEM specimen stubs. The specimen stubs were subjected to gold coating of 4 nm thickness by ion sputtering device (Au5 Quorum, Q150TES) and were operated at 15-20 kV accelerating voltage.

3.2.3.4. Transmission electron microscopy (TEM)

The internal surface and drug distribution in the developed nanoparticles were examined employing transmission electron microscope at the operating voltage 200 KV, and resolution 0.19 nm (Model: JEOL 2100, FEI, Czech Republic). The nanoparticle suspension in Milli Q water was dropped on standard carbon coated copper grid (mesh) and air dried for 5 h (Paul et al., 2018). TEM images were taken and analysed.

3.2.3.3. Atomic force microscopy (AFM)

The samples were dispersed in Milli-Q water by brief vortexing. One drop of sample was placed in a glass slide and dried in a vacuum dryer (Paul et al., 2018). The morphology and particle size were analyzed by atomic force microscopy (AFM; Model Solver Pro, Bruker, Karlsruhe, Germany) under ambient conditions by mode PeakForce QNM (Quantitative NanoMechanical mapping) using silicon nitride probe having a resonance frequency 150-350 kHz and a force constant 0.4 N/m.

3.2.3.4. Drug release (DR) study

DR from the nanoparticles was studied in PBS (pH 7.4) or release medium (Sinha et al. 2013). 2 mg of formulation were taken in a 2 ml eppendorf tube and 2 ml of release medium was added to the eppendorf tube (Sinha et al., 2013). The samples were kept under slow shaking condition (120/min) at 37°C in an incubator shaker (Sinha et al. 2013). After the scheduled time intervals, the tubes were centrifuged and the supernatant were collected (Sinha et al. 2013). A volume of 1 ml of the fresh release medium was added in the sample tube (Sinha et al. 2013). Then the collected samples were analysed spectrophotometrically at 210 nm (Sinha et al. 2013).

3.2.3.5. Kinetics of release study

The release study of all the formulations fitted with zero order, first order, Higuchi, Hixson Crowell, and Korsmeyer-Peppas models to find out the drug release kinetics (Dash et al., 2010).

Zero order equation

The pharmaceutical dosage forms following zero order kinetics, release the same amount of drug by unit of time and it is the ideal method of drug release in order to achieve a prolonged pharmacological action (Dash et al., 2010). For this model, a graph of percent drug released versus time will be linear (Dash et al., 2010). The following relation (4) can in a simple way express this model (Dash et al., 2010).

$$Q_t = k_0.t \quad \text{.....(4)}$$

Where, Q_t is the amount of drug released in time t, Q_0 is the initial amount of drug in the solution and K_0 is the zero order release rate constant (Dash et al., 2010).

First order equation

The pharmaceutical dosage forms following this kinetics profile, such as those containing water soluble drugs in porous matrices release the drug in a way that is proportional to the amount of drug released by unit of time diminishes (Reddy., 2014). This model can be expressed from equation (5).

$$Q_t = e^{-K}{}_1.t \quad \text{.....(5)}$$

Where, Q_t is the amount of drug released at time t, Q_0 is the initial amount of drug in the solution and K_1 is the first order release rate constant (Reddy., 2014)..

Higuchi's equation (6)

$$Q_t = K_H.t_{1/2} \quad \text{.....(6)}$$

Where, K_H is the Higuchi release rate constant (Reddy, 2014).

Hixson-Crowell equation (7)

$$Q_0^{1/3} - Q_t^{1/3} = K_{HC}.\ t \quad \text{.....(7)}$$

Where K_{HC} is the Hixson Crowell rate constant (Reddy., 2014).

Korsmeyer-Peppas Equation (8)

In order to better characterize the drug release mechanisms from the polymeric systems studied, the Korsmeyer-Peppas "Semi-empirical model" was applied (Korsmeyer et al. 1983).

$$Q_t/Q_\infty = k_{KP}.\ t^n \quad \text{.....(8)}$$

Where, Q_t/Q_∞ is the fraction of drug release at time t, K_{kp}, a constant compromising the structural and geometric characteristics of the device, and n, the release exponent, which is indicative of the mechanism of drug release (Korsmeyer et al., 1983). When, n = 0.45 it corresponds to a Fickian diffusion release (Case I); when the n value is $0.45 < n < 0.89$ it corresponds to a non-Fickian (anomalous) transport, n = 0.89 describes to a zero order (Case II) release kinetics (Siepmann et al., 2001) and $n > 0.89$ corresponds to a super Case II transport (Vueba et al., 2004).

3.2.4. Data analysis

The experimental data were analyzed using computerized GraphPad InStat (version 3.05), GraphPad software, USA. The data were denoted as mean ± SD.

Chapter 4

Results

Contents

4. Results

4.1. Determination of drug loading and drug entrapment efficiency

4.1.1. Asiatic acid standard curves

Asiatic acid in PLGA nanoparticles was determined by UV-spectrophotometric method. Drug absorbance at y-axis was plotted against drug concentration in ethanol at x-axis and the calibration curve was drawn (Figure 4.1.). The linear equation of the calibration curve was found to be y = 0.026x, with a correlation coefficient of 0.9985.

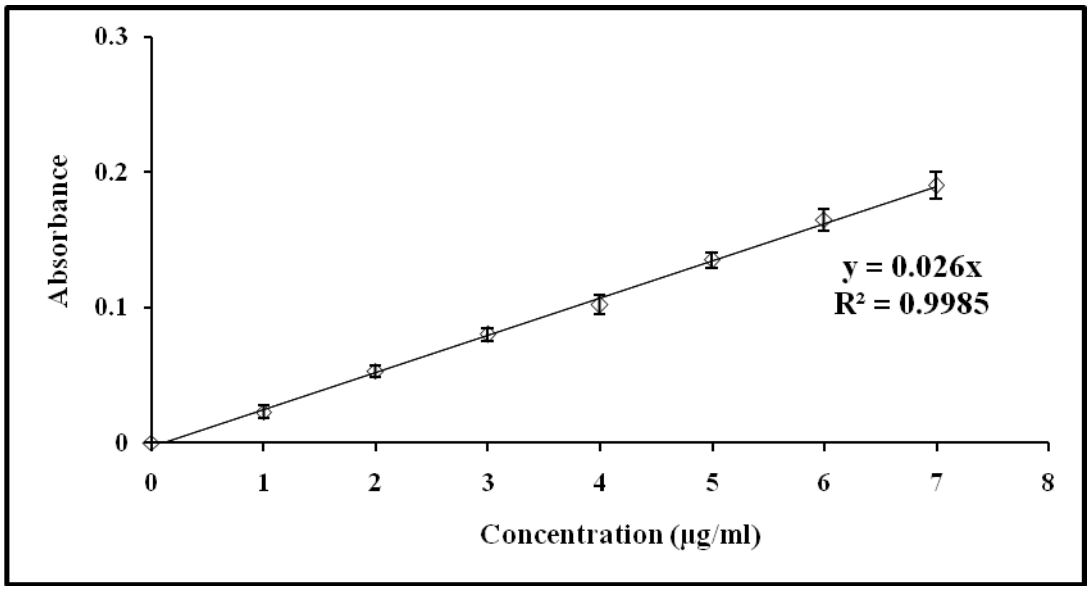

Figure 4.1. Calibration curve of asiatic acid in ethanol.

Date were expressed mean ± SD (n = 3).

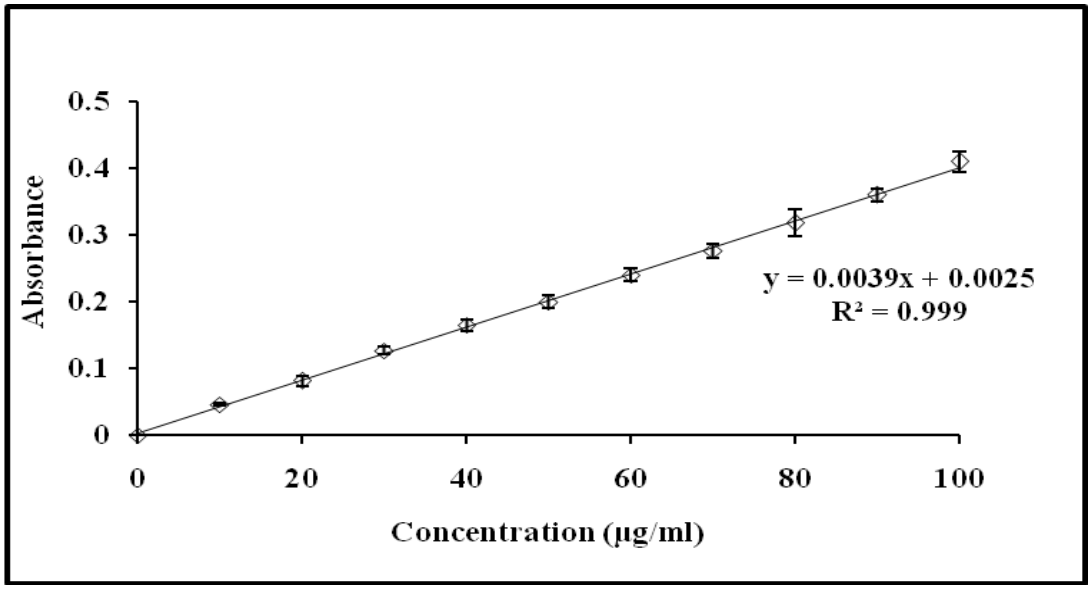

Figure 4.2. Calibration curve of asiatic acid in PBS buffer.

Date were expressed mean ± SD (n = 3).

Asiatic acid in PLGA nanoparticles was also determined by plotting absorbance at y-axis against drug concentration in PBS buffer at x-axis and the calibration curve was drawn (Figure 4.2). The linear equation of the calibration curve obtained was found to be y = 0.004x + 0.0025, with a correlation coefficient of 0.999.

4.1.2. Determination of drug loading and drug entrapment

Drug loading in asiatic acid loaded nanoparticles in drug: PLGA ratio of 1:10 was found to be 6 % and the theoretical drug loading in the formulation was found to be 9.09 %. Approximate drug: PLGA ratio of 1:10 exhibited best entrapment efficiency of asiatic acid in the formulation, in which drug entrapment efficiency in asiatic acid nanoparticle was found to be 66.01 % (Table 4.1.).

Table 4.1. Compositions and (%) drug entrapment efficiency of nanoparticles.

Drug to polymer ratio	Amount of drug (mg)	Amount of polymer, PLGA (85:15) (mg)	Entrapment efficiency (%)
1:3	5	15	24
1:6	5	30	42
1:10	5	50	66.01

4.2. Drug-excipient interaction study

4.2.1. ATR spectroscopy

Figure 4.3. showed the ATR spectra of asiatic acid, PLGA, PVA, their physical mixtures and the prepared lyophilized formulation without and with drug. The ATR spectra of pure asiatic acid, mixture of drug with the polymers and PVA and the lyophilized formulations with or without drug show that the characteristic peaks of O-H, -CH_3, -COOH and C=C at 3872-3395, 1458, 2967-2879 and 1687 cm^{-1}, respectively, which revealed the presence of asiatic acid in nanoparticles (Figure 4.3.a, e, and f) . In the ATR spectrum of PLGA, sharp peaks at 3989–2613 cm^{-1} for –OH (free) and of 2467 cm^{-1} for C–H stretching were observed as the typical bands of PLGA (Figure 4.3.b). The ester C–O stretching band of PLGA was observed at 1794.61 cm^{-1} (Figure 4.3.b). Data revealed that all the typical bands of PLGA and asiatic acid were present in the ATR spectrum of their physical mixture and the presence of the characteristic peaks of drug and the excipients in the formulations were observed (Figure 4.3.a, e, and f). Furthermore, when ATR spectra of the physical mixture of asiatic acid and the excipients were compared, no

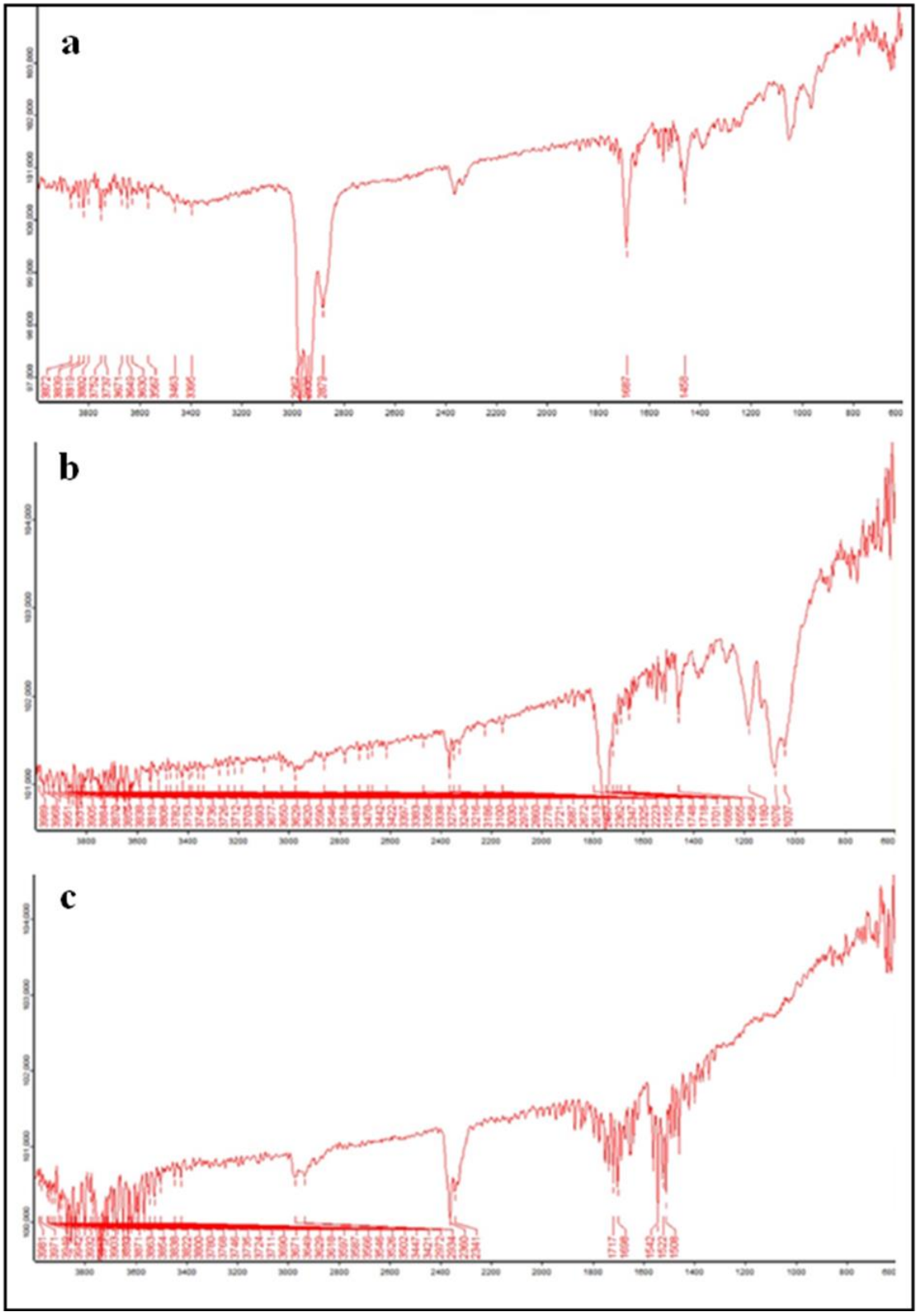
a
b
c

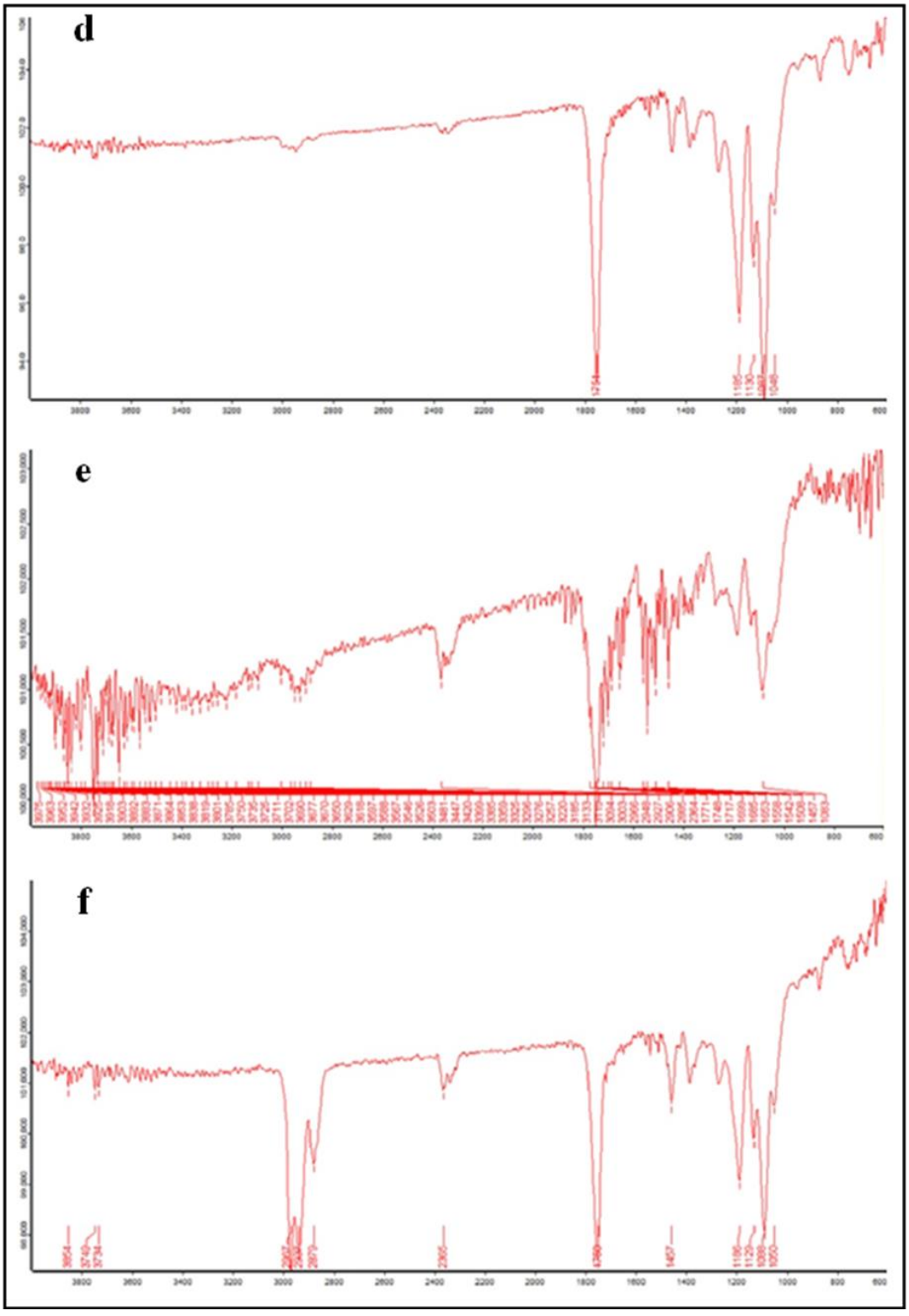

Figure 4.3. ATR spectrum of asiatic acid (a), PLGA (b), PVA (c), lyophilized PLGA-PVA (d), lyophilized PLGA-PVA-asiatic acid (e), formulated nanoparticles (f).

shifting of predominant peaks of the drug and the excipients was found, suggesting no chemical interaction has taken place. However, few minor shiftings of peaks of the excipients were detected in the wave numbers from 940 cm^{-1} to 920 cm^{-1} responsible for

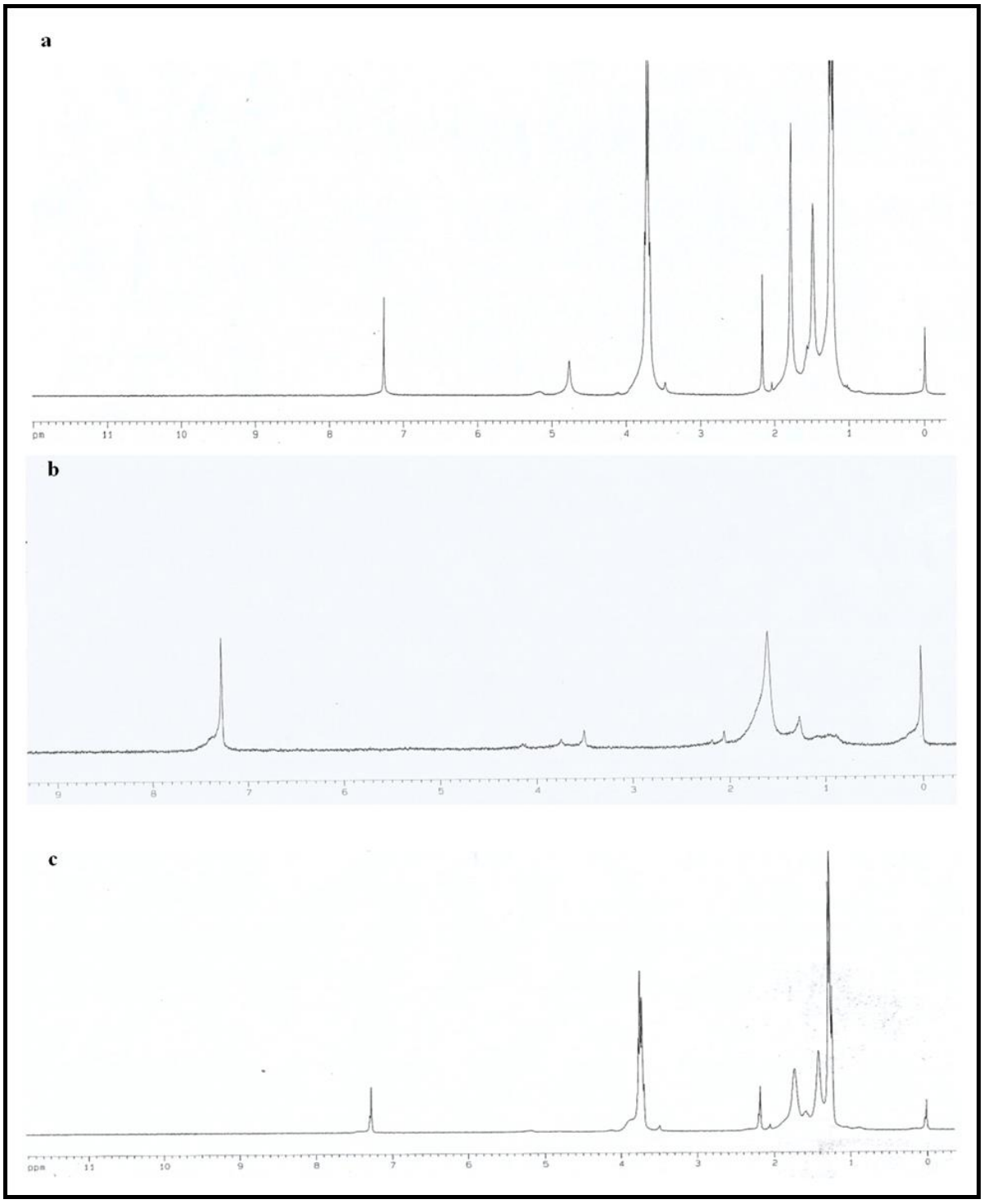

Figure 4.4. ^{1}H-NMR of asiatic acid (a), PLGA (b), asiatic acid-PLGA mixture (c).

alkane, from 3406 cm^{-1} to 3402 cm^{-1} responsible for benzene ring or substituted benzene, and at 3435 cm^{-1} responsible for -OH group (Figure 4.3.e, f). The shifting of such peaks might have taken place due to the weak physical interactions such as formation of weak H-bonding, van der Waal's force of attraction, dipole-dipole interaction between the various functional groups of asiatic acid, PLGA and PVA molecules (Paul et al., 2018). The physical interaction might be responsible for the formation of spherical structure of the nanoparticles (Paul et al., 2018). Presence of drug peak in the lyophilized formulations suggests that some drug molecules were present on the surface (Paul et al., 2018).

4.2.2. NMR spectroscopy

In this study, the ^{1}H-NMR spectra of asiatic acid, PLGA, and asiatic acid-PLGA mixture were shown in Figure 4.4. The ^{1}H-NMR spectra of asiatic acid (Figure 4.4.a) and PLGA (Figure 4.4.b) established their structural identities. On the other hand, ^{1}H-NMR spectra of asiatic acid-PLGA mixture did not exhibit the appearance of any new peak of proton or any change in shift or any change in peak pattern (Figure 4.4.c), which revealed the chemical compatibility between asiatic acid and PLGA.

4.3. Particle size determined by DLS technique

Particle size of nanoparticle was also determined by dynamic light scattering technique shown in Figure 4.5 to corroborate the particle size obtained by field emission scanning electron microscopy. The particle size distribution of the formulation was 250-470 nm (average particle size was 360 nm) with the poly-dispersity index (PDI) of 0.071.

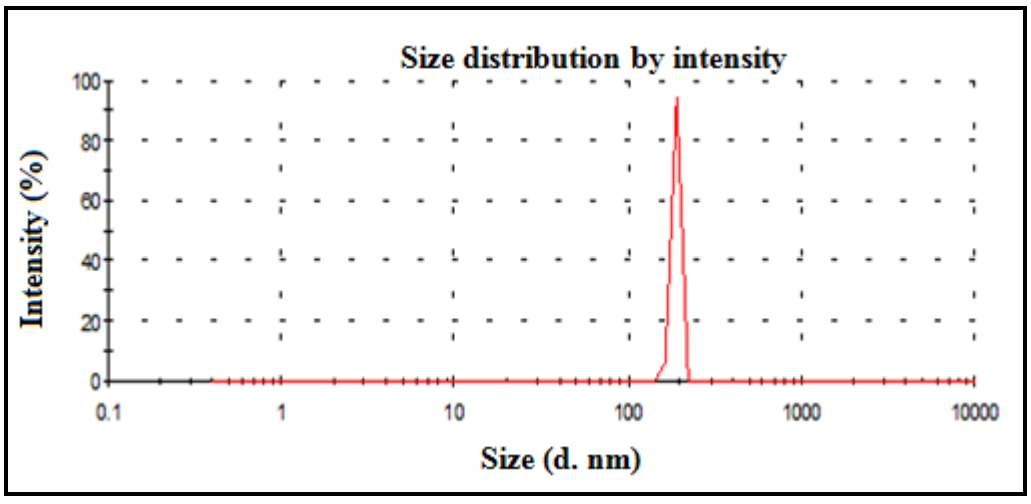

Figure 4.5. Zetasizer analysis data of formulation (360 nm) showing the particle size distribution.

4.4. Zeta Potential Determination

The zeta potential of the formulation is -12.0 mV. The zeta potential describes the nature of the electrostatic potential at the surface of a particle (Dey et al., 2016). An absolute zeta potential value of –30 mV to +30 mV suggests that the particles would remain in suspended state for a longer period and are not susceptible for quick agglomeration in the liquid state (Meißner et al. 2009; Basu et al. 2012). Thus, the repulsion among the negatively charged asiatic acid loaded nanoparticles provide stability and prevents aggregation (Honary and Zahir, 2013).

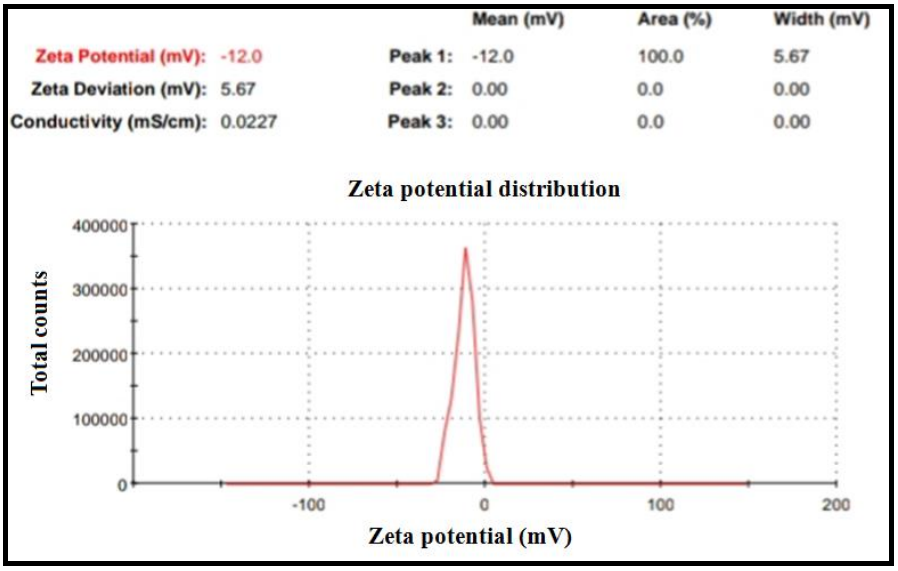

Figure 4.6. Zeta potential (-12.0 mV) of asiatic acid nanoparticles.

4.5. Determination of particle surface morphology using FE-SEM

The morphology of lyophilized PLGA based asiatic acid nanoparticles was exhibited by FE-SEM photographs in Figure 4.7. Prepared nanoparticles were submicron in size (200 nm) and spherical in shape, possessing smooth surface.

4.6. Determination interior morphology using TEM

TEM of asiatic acid-PLGA nanoparticles examined the interior structure of nanoparticles (Figures 4.8.). These nanoparticles (200 nm) are spherical in shape with smooth surface. There was homogeneous molecular distribution of drug in the polymer based nanoparticles.

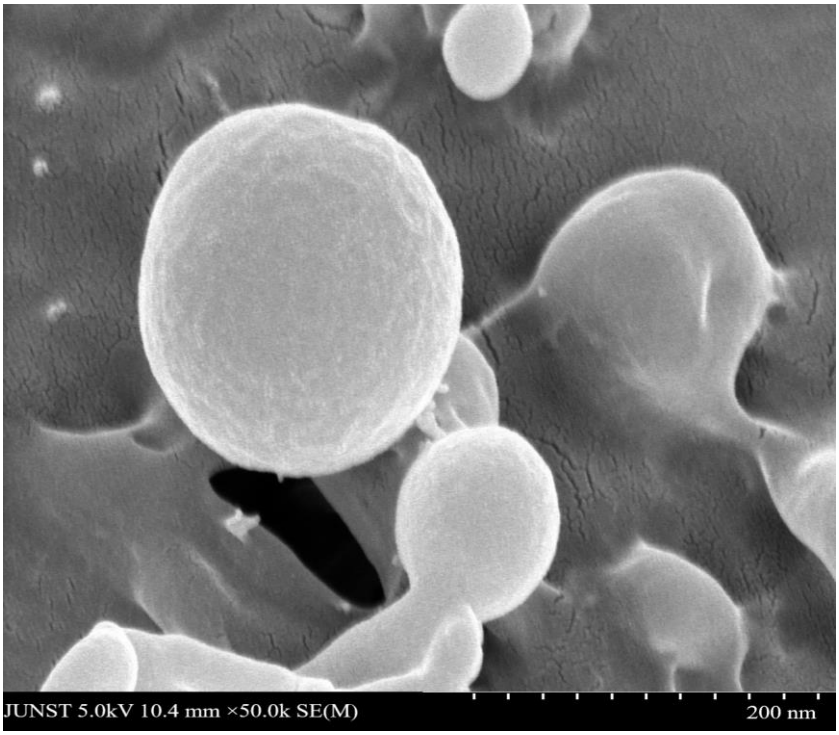

Figure 4.7. FE-SEM images of developed nanoparticles.

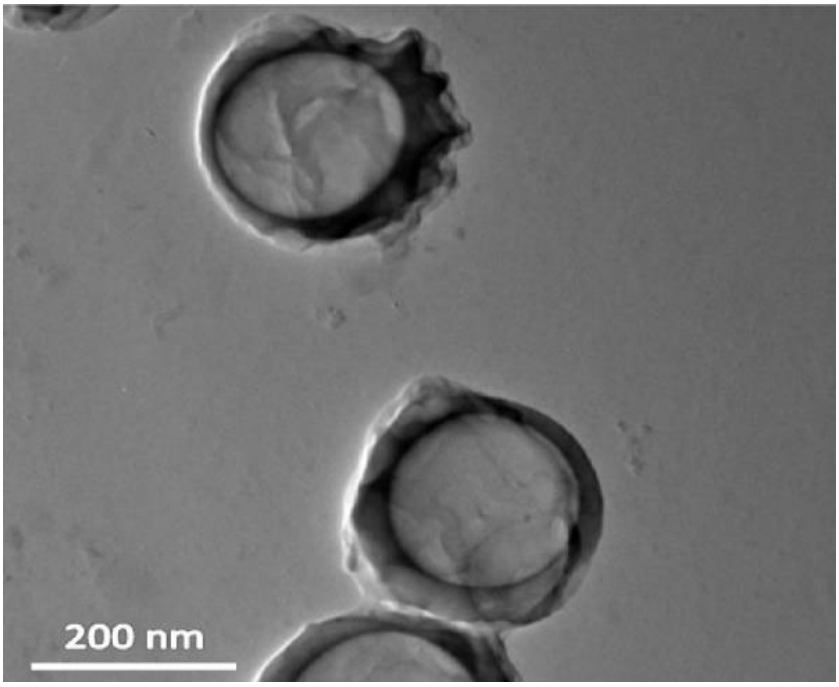

Figure 4.8. TEM image of developed nanoparticles.

4.7. AFM study

In the AFM of the formulation, we can see the 3D view of the nanoparticles (Figure 4.9.a). The morphological studies performed by AFM showed uniform and purely spherical shaped discrete particles without aggregation and smooth in surface

morphology (Figure 4.9.a). Line analysis of AFM image using SPM software revealed that the particle sizes of nanoformulation reside between 300 and 500 nm (Figure 4.9b).

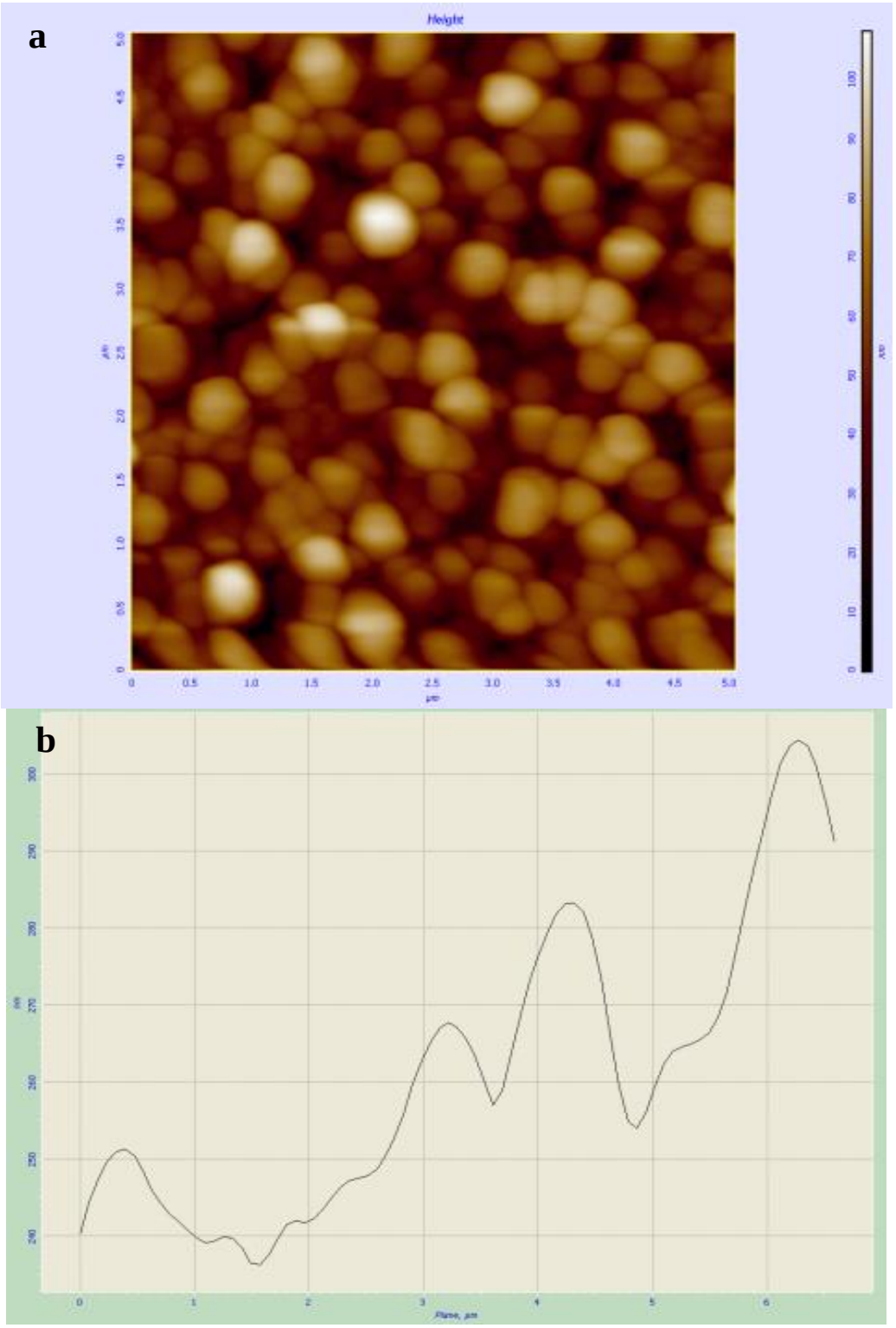

Figure 4.9. 3D view of the nanoparticles in atomic force microscopy (a). 2D line from the same scanned area (b).

Table 4.2 depicted the numerical values of overall characteristic features of developed asiatic acid-PLGA nanoparticles obtained from various physic-chemical characterization studies.

Table 4.2. Formulation characteristics such as percent drug loading, percent encapsulation efficiency, average particle size, average particle size, PDI, zeta potential, FE-SEM, TEM and AFM values for the optimized asiatic acid-PLGA nanoparticles.

Characterization of Formulation	**Values**
Drug Loading (%)	6
Entrapment Efficiency (%)	66.01
Average particle size (nm)	360
PDI	0.071
Zeta Potential (mV)	-12
Particle size (nm) from FE-SEM	200
Particle size (nm) from TEM	200
Particle size (nm) from AFM	300-500

4.8. In vitro drug release study

Drug release study was carried out to understand in vitro drug release pattern from the nanoparticles formulations. A sustained drug release pattern was observed. After 216 h, the cumulative % of in vitro release of asiatic acid was found to be 81.84 % from the nanoparticle formulation. To evaluate the drug-release, drug release data were assessed using zero order (4.10a), first order (4.10b), Korsmeyer Peppas (4.10c), Hixson-Crowell (4.10d), and Higuchi kinetic models (4.10e) (Rudra et al, 2010). Calculated R^2 values for the kinetics were tabulated (Table 4.3.). The corresponding plot (log cumulative percent drug release vs. log time) for the Korsmeyer-Pappes equation indicates a good linearity (R^2 = 0.9651) for the formulation and the release exponent ("n" value) for the formulation was found to be 0.49.

Table 4.3. R^2 values of different drug release kinetics models of the formulation

Different Drug Release Kinetics Models	**Correlation coefficient (R^2)**	**Release exponent (n)**
Zero order	0.8929	-
First order	0.8929	-

Hixson-Crowell	0.7601	-
Higuchi	0.9607	-
Korsmeyer-Peppas	0.9651	0.49

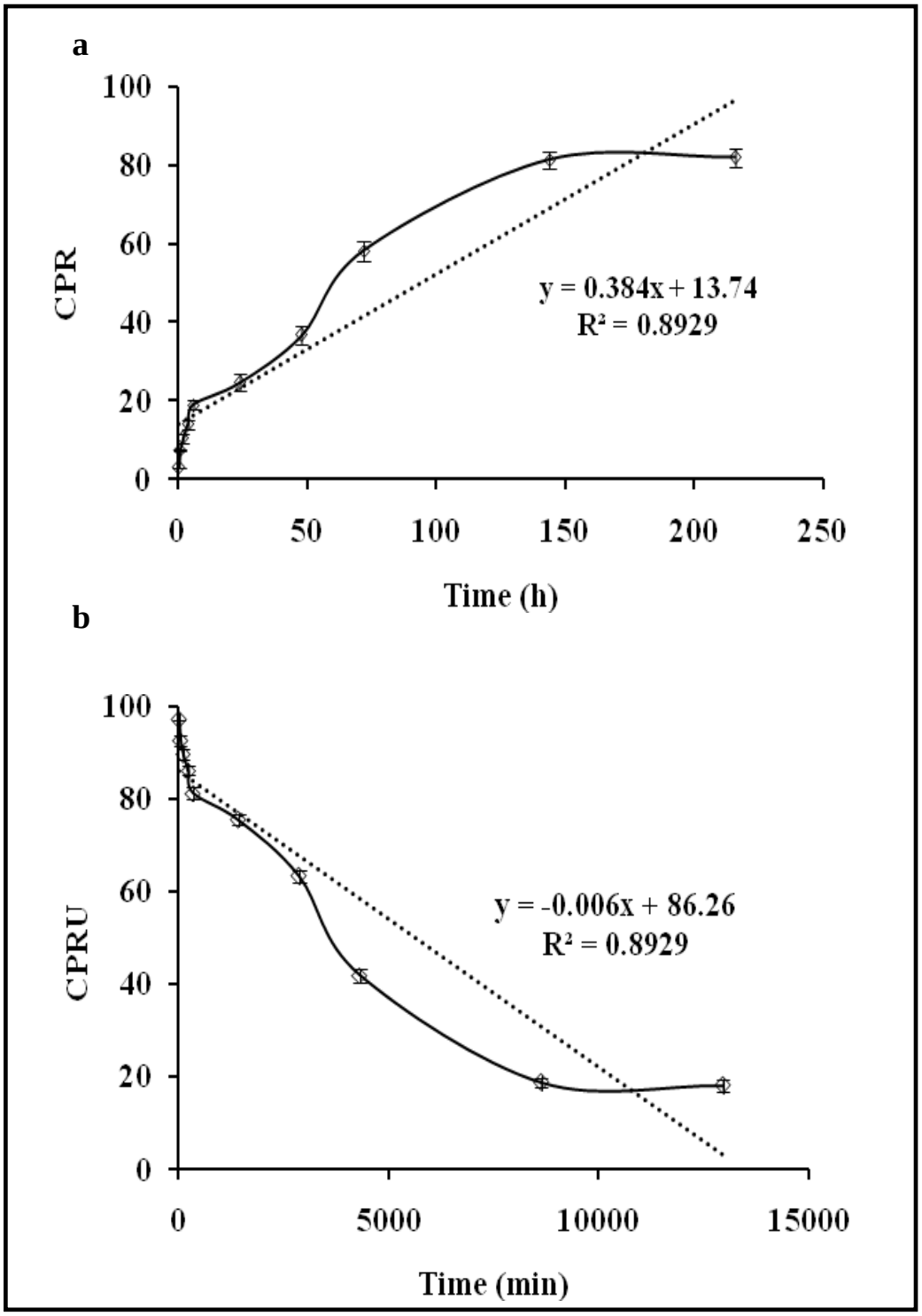

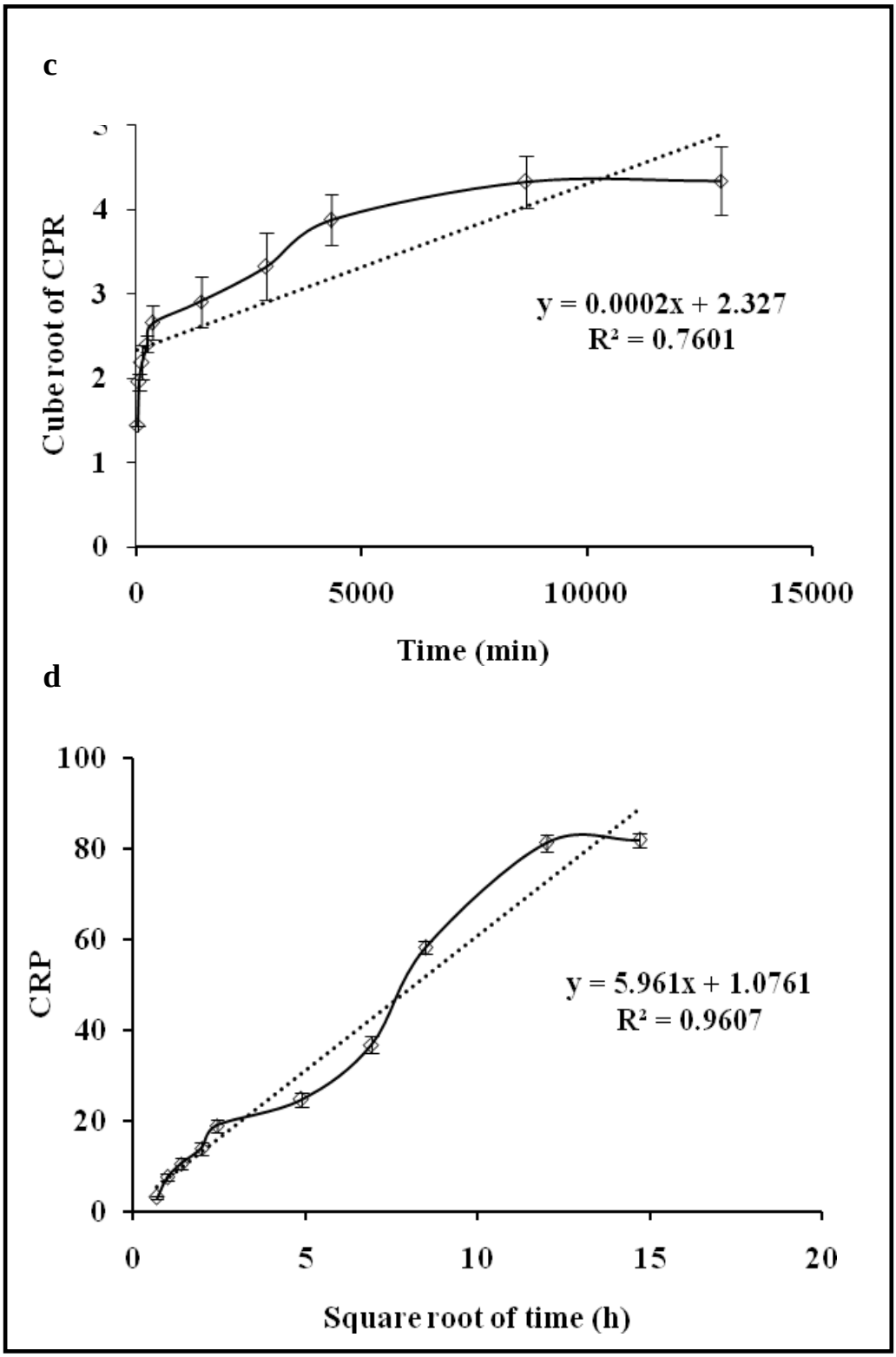
c
Cube root of CPR
0
1
2
3
4
y = 0.0002x + 2.327
R² = 0.7601
0
5000
10000
15000
Time (min)
d
CRP
0
20
40
60
80
100
y = 5.961x + 1.0761
R² = 0.9607
0
5
10
15
20
Square root of time (h)

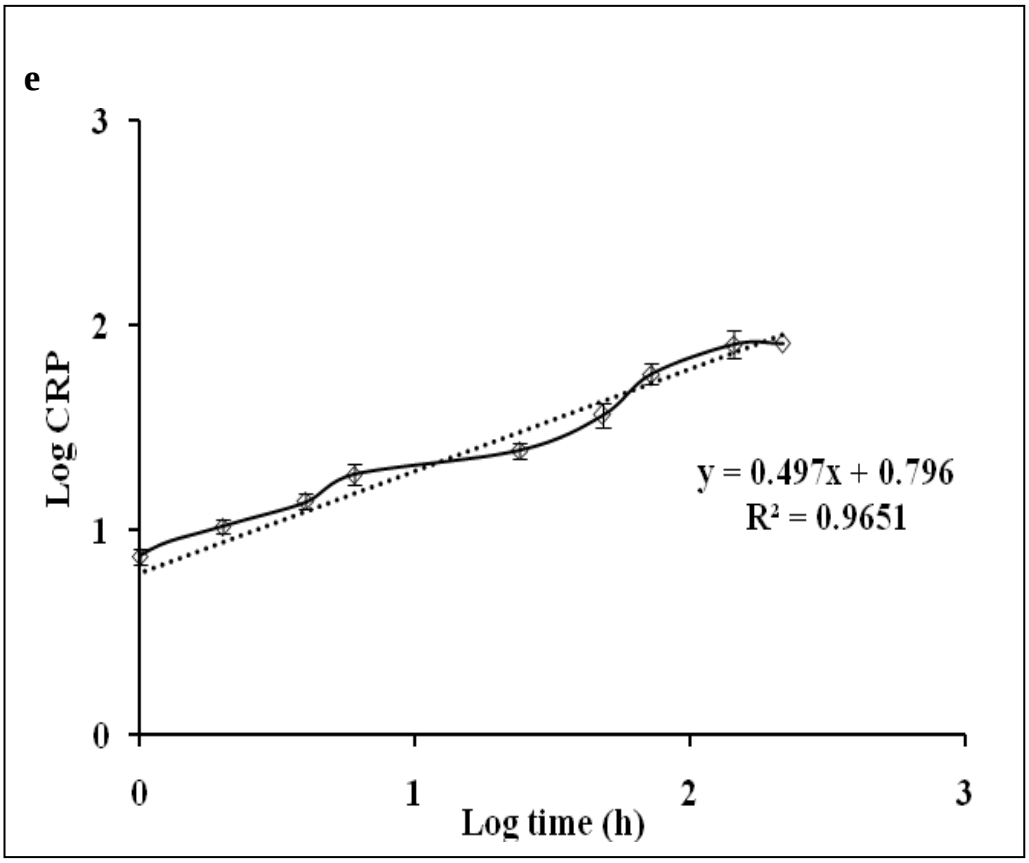

Figure 4.10. Drug release kinetics plots zero order plot (a), first order plot (b), Hixson-Crowell plot (c), Higuchi plot (d), and Korsmeyer-Peppas plot (e).

Chapter 5

Discussion

5. Discussion

In this study, US-FDA-approved biodegradable polymer (PLGA)-based asiatic acid nanoparticles have been formulated. Asiatic acid possesses poor bioavailability as it undergoes rapid metabolism (Meeran et al., 2018). Therefore, asiatic acid-loaded nanoparticles were formulated in this project work to improve the bioavailability of the drug. To achieve this objective, PLGA-based asiatic acid nanoparticles were formulated using multiple emulsions and solvent evaporation method. The characterizations of the developed nanoparticles were performed through particle size analysis, surface morphology assessment, drug distribution study, drug-excipients incompatibility assessment, and in vitro drug release study in this project work.

Asiatic acid showed a sharp UV-absorbance peaks (λ_{max}) at 210 nm. At the beginning, drug-excipient interaction was studied using ATR spectroscopic technique. Data revealed that all the typical bands of PLGA and asiatic acid were present in the ATR spectrum of their physical mixture and the presence of the characteristic peaks of drug and the excipients in the formulations were observed. Furthermore, when ATR spectra of the physical mixture of asiatic acid and the excipients were compared, no shifting of predominant peaks of the drug and the excipients was found, suggesting no chemical interaction has taken place. However some physical interactions between the drug and the mixture of the excipients were observed. This might be due to the formation of weak bonds such as weak hydrogen bonding, van der Waal's force of attraction, dipole-dipole interaction between the various functional groups of asiatic acid, PLGA and PVA molecules (Paul et al., 2018). The physical interaction might be responsible for the formation of spherical structure of the nanoparticles (Paul et al., 2018). Presence of drug peak in the lyophilized formulations suggests that some drug molecules were present on the surface (Paul et al., 2018). The possible interactions between asiatic acid and excipients have been estimated by the NMR spectroscopic analysis of asiatic acid, PLGA and their physical mixture, respectively. No interaction was found in the NMR spectrum of the asiatic acid and PLGA mixture.

PLGA has been a most attractive polymeric candidate to fabricate nanonoparticle-based drug delivery. Several studies mentioned the success of PLGA-based nanoparticle formulations (Averineni et al., 2012; Danhier et al., 2012; Paul et al., 2018). However, we followed the method described by Paul and co-workers (2018) to develop asiatic acid nanoparticles. In this study, the asiatic acid nanoparticles were prepared by multiple

emulsion and solvent evaporation method and PLGA (85:15) has been used to develop PLGA-asiatic acid nanoparticles. Asiatic acid and DMSO mixture was present in DCM and acetone along with the PLGA in the primary emulsion (W/O). This primary emulsion was further emulsified in the 1.5% PVA solution to prepare W/O/W emulsion. Presence of stable drug molecules within the formulation has been detected by the ATR and NMR study.

Drug-polymer ratio has been optimized to achieve the maximum drug entrapment efficiency in the developed nanoparticles and the drug-polymer ratio (1:10) has been established optimum to achieve maximum entrapment of asiatic acid in the developed formulation.

Four different methods, namely, DLS, FESEM, AFM and TEM were adopted to reveal the particle size, particle size distribution, surface morphology, interior structure, and drug distribution in the PLGA-asiatic acid nanoparticles. The FE-SEM images of the prepared nanoparticles showed that all the prepared nanoparticles were spherical in shape, having smooth surface. The particles were found to be in submicron size with a relatively narrow range of distribution as supported by the PDI values. The particle size obtained from FE-SEM was further supported by the particle size measured by DLS method. The average particle sizes of the formulations varied from 250-470 nm. Sizes of the lyophilized particles observed in FE-SEM were found to be smaller than those detected by DLS. The difference in size may be because of the DLS method, which measures the average hydrodynamic diameter of nanoparticles in aqueous suspension where the particles might swell and increase in size (Yu et al., 2010). Size analysis data by DLS showed that the average size (Z-average) of nanoparticles was 360 nm.

In the AFM of the formulation, we can see the 3D view of the nanoparticles. AFM showed that the nanoparticles are morphologically uniform and purely spherical shaped discrete particles without aggregation with a nano size range of 300-500 nm. In addition, the nanoparticles exhibit a smooth in surface morphology. Line analysis of AFM image revealed the size of the particles remain within nano-range of 300-500 nm.

TEM analysis of asiatic acid loaded nanoparticles revealed the interior diameter of nanoparticles of 200 nm. These nanoparticles have spherical in shape, having smooth internal surface. There was homogeneous molecular distribution of drug within the polymer based nanoparticles.

The zeta potential of a particle indicates the overall charge that particles acquire in a particular medium and at a particular temperature (Averineni et al., 2012). The zeta

potential describes the nature of the electrostatic potential at the surface of a particle (Averineni et al., 2012). The physical stability of particles can also be predicted from their zeta potential value. An absolute zeta potential value between -30 mV and +30 mV suggests that the particles would remain in suspended state for a longer period and are not susceptible for quick agglomeration in the liquid state (Meißner et al. 2009; Basu et al. 2012; Dey et al., 2016). The zeta potential of the formulation is -12.0 mV. Presence of terminal carboxyl group in the PLGA polymer provided negative surface charge to the nanoparticles (Sun et al., 2015). Thus, the repulsion among the negatively charged nanoparticles provides stability and prevents aggregation (Honary and Zahir, 2013).

In vitro release of asiatic acid was observed over a period of 216 h from the developed formulation. The cumulative release of 81.84 % of asiatic acids from the formulation was seen in 216 h. The data of percentage drug release formulation were calculated using different kinetic equations and plotted as cumulative % drug release vs. time (zero order kinetic model), log cumulative % drug remaining vs time (first order kinetic model), cube root of cumulative % drug release vs time (Hixson-Crowell), cumulative % drug release vs square root of time (Higuchi model), and log cumulative % drug release vs log time (Korsmeyer-Peppas model). On the basis of best fit with the highest correlation (R^2) value, it was concluded that in the optimized formulation of nanoparticles follow the Korsmeyer-Peppas model with release exponent value $n = 0.49$. When $n = 0.45$, it corresponds to a Fickian diffusion release (Case I); when the n value is $0.45 < n < 0.89$ it corresponds to a non-Fickian (anomalous) transport; $n = 0.89$ describes to a zero order (Case II) release kinetics (Siepmann and Peppas, 2001); and $n > 0.89$ corresponds to a super Case II transport (Vueba et al. 2004). So, in this study, the magnitude of the release exponent "n" indicates the release mechanism is non-Fickian diffusion. More linearity (as assessed by R^2 values) of drug release data toward Korsmeyer-Peppas kinetics implies anomalous diffusion controlled drug release by more than one process. Due to long-term slow degradation of PLGA, release of drug molecules follows a coupling of diffusion and erosion mechanism for PLGA degradation by slow hydrolysis of ester linkage in three phases (Mukherjee et al. 2010). The three predominant sequences by which PLGA degrades are: random polymeric chain scission causing a decrease in molecular weight without much loss of molecular weight along with the formation of soluble monomers; a decrease in polymeric molecular weight with a rapid loss of mass due to the formation of oligomers and soluble monomers; and the conversion of soluble

oligomers into soluble monomers causing complete solubilisation (Mukherjee et al. 2010). This ultimately causes to anomalous drug diffusion.

Chapter 6

Conclusion

6. Conclusion

Nanoparticles have advantages over conventional formulations as the bioavailability, solubility and permeability of many potent drugs can be orchestrated through developing their nanoformulations. Asiatic acid is a sapogenin with various therapeutic applications. However, it possesses poor oral bioavailability due to its rapid metabolism, which is a major concern with asiatic acid in conventional dosage forms. This project work aimed to formulate the PLGA-based asiatic acid nanoparticles to improve the bioavailability of asiatic acid. The developed asiatic acid-PLGA nanoparticles were spherical in shape offering smooth outer surface. The particle size was found to be < 600 nm. The developed formulation was quite stable and did not exhibit any sign of drug-excipient incompatibility. Moreover, asiatic acid-PLGA nanoparticles showed significant quantity of sustained drug release from the formulation in vitro. Therefore, it may be claimed that asiatic acid nanoparticles would be a potential formulation for subjecting to pre-clinical studies to evaluate their therapeutic efficacy over conventional formulation and free drugs.

References

References

Akbarzadeh A, Rezaei-Sadabady R, Davaran S, et al. Liposome: classification, preparation, and applications. Nanoscale Res. Lett. 2013;8(102):1-9.

Averineni RK, Shavi GV, Gurram AK. PLGA 50:50 nanoparticles of paclitaxel: development, in vitro anti-tumor activity in BT - 549 cells and in vivo evaluation. Bull. Mater. Sci. 2012;35(3):319-326.

Baer DR, Engelhard MH, Johnson GE, et al. Surface characterization of nanomaterials and nanoparticles: Important needs and challenging opportunities. J Vac Sci Technol A. 2013;31(5):50820. doi:10.1116/1.4818423.

Bailey R, Nie S. Alloyed semiconductor quantum dots: tuning the optical properties without changing the particle size. J. Am. Chem. Soc. 2003;125(23):7100-7106.

Bamrungsap S, Zhao Z, Chen T, et al. Nanotechnology in therapeutics: a focus on nanoparticles as a drug delivery system. Nanomedicine. 2012;7(8):1253-1271.

Basu S, Mukherjee B, Chowdhury SR, Paul P, Choudhury R, Kumar A, Mondal L, Hossain CM, Maji R. Colloidal gold-loaded, biodegradable, polymer-based stavudine nanoparticle uptake by macrophages: An *in vitro* study. Int J Nanomedicine. 2012;7:6049–6061.

Bazak R, Houri M, Achy SE, Hussein W, Refaat T. Passive targeting of nanoparticles to cancer: A comprehensive review of the literature. Mol Clin Oncol. 2014;2(6):904-908.

Bhatia S. Nanoparticles types, classification, characterization, fabrication methods and drug delivery applications. Natural Polymer Drug Delivery Systems. 2016; 33-93.

Bosi S, Da Ros T, Spalluto G, Prato M. Fullerene derivatives: an attractive tool for biological applications. Eur. J. Med. Chem. 2003;38(11 -12):913-923.

Callaghan R, Luk F, Bebawy M. Inhibition of the multidrug resistance P-glycoprotein: time for a change of strategy?. Drug Metab Dispos. 2014;42(4):623–631. doi:10.1124/dmd.113.056176.

Chen H, Hua XM, Ze BC, Wang B, Wei L. The anti-inflammatory effects of asiatic acid in lipopolysaccharide-stimulated human corneal epithelial cells. Int J Ophthalmol. 2017;10(2):179-185.

Chen Z, Ma L, Liu Y, Chen C. Applications of functionalized fullerenes in tumor theranostics. Theranostics. 2012;2(3):238-250.

Danhier F, Ansorena E, Azeitao J. PLGA-based nanoparticles: An overview of biomedical applications. J Control Release. 2012;161:505-522.

Das PJ, Paul P, Mukherjee B. Pulmonary delivery of voriconazole loaded nanoparticles providing a prolonged drug level in lungs- a promise for treating fungal infection. Mol. Pharm. 2015;12(8):2651-2664.

Dash S, Murthy PN, Nath L, Chowdhury P. Kinetic modelling on drug release from controlled drug delivery systems. Acta Pol Pharm. 2010; 67(3):217-223.

De Jong W, Borm P. Drug delivery and nanoparticles: applications and hazards. Int. J. Nanomedicine. 2008;3(2):133-149.

Dey NS, Mukherjee B, Maji R, Satapathy BS. Development of linker-conjugated nanosize lipid vesicles: a strategy for cell selective treatment in breast cancer. Curr. Cancer Drug Targets. 2016;16(4):357–372.

Dimitrakopoulos FI, Kottorou A, Antonacopoulou AG, Makatsoris T, Kalofonos HP. Early-stage breast cancer in the elderly: confronting an old clinical problem. J. Breast Cancer. 2015;18:207-217.

Din FU, Aman W, Ullah I. Effective use of nanocarriers as drug delivery systems for the treatment of selected tumors. Int J Nanomedicine. 2017;12:7291-7309.

Dinarvand R, Sepehri N, Manoochehri S, Rouhani H, Atyabi F. Polylactide-co-glycolide nanoparticles for controlled delivery of anticancer agents. Int J Nanomedicine. 2011;6:877.

Dubertret B, Skourides P, Norris D, Noireaux V, Brivanlou A, Libchaber A. In vivo imaging of quantum dots encapsulated in phospholipid micelles. Science. 2002;298(5599):1759 -1762.

Ediriwickrema A, Saltzman WM. Nanotherapy for cancer: targeting and multifunctionality in the future of cancer therapies. ACS Biomater Sci Eng. 2015;1(2):64-78.

Fernandez-Fernandez A, Manchanda R, McGoron A. Theranostic applications of nanomaterials in cancer: drug delivery, image-guided therapy and multifunctional platforms. Appl Biochem Biotechnol. 2012;165(7-8):1628-1651.

Fong LY, Ng CT, Cheok ZL, Mohd Moklas MA, Hakim MN, Ahmad Z. Barrier protective effect of asiatic acid in TNF-α-induced activation of human aortic endothelial cells. Phytomedicine. 2016 ;23(2):191-199.

Gaaz TS, Sulong AB, Akhtar MN, Kadhum AAH, Mohamad AB, Amiery AAA. Properties and applications of polyvinyl alcohol, halloysite nanotubes and their nanocomposites. Molecules. 2015; 20: 22833-22847.

Gao X, Cui Y, Levenson R, Chung L, Nie S. In vivo cancer targeting and imaging with semiconductor quantum dots. Nat. Biotechnol. 2004;22(8):969-976.

Ghasemi Y, Peymani P, Afifi S. Quantum dot: magic nanoparticle for imaging, detection and targeting. Acta Biomed. 2009;80(2):156-165.

Gurfinkel DM, Chow S, Hurren R, Gronda M, Henderson C. Disruption of the endoplasmic reticulum and increases in cytoplasmic calcium are early events in cell death induced by the natural triterpenoid Asiatic acid. Apoptosis. 2006;11:1463-1471.

Honary S, Zahir F. Effect of zeta potential on the properties of nano- drug delivery systems–a review (part1). Trop. J. Pharm. Res. 2013;12:255-264.

Hou W, Li Y, Zhang Q, Wei X, Peng A, Chen L. Triterpene acids isolated from Lagerstroemia speciosa leaves as a-glucosidase inhibitors. Phytother. Res. 2009;23:614-618.

Hsu YL, Kuo PL, Lin LT, Lin CC. Asiatic acid, a triterpene, induces apoptosis and cell cycle arrest through activation of extracellular signal-regulated kinase and p38 mitogen-activated protein kinase pathways in human breast cancer cells. J. Pharmacol. Exp. Ther. 2005;313:333-344.

Hu Y, Fu L. Targeting cancer stem cells: a new therapy to cure cancer patients. Am J Cancer Res. 2012;2(3):340-356.

Hung YC, Yang HT, Yin MC. Asiatic acid and maslinic acid protected heart via anti-glycative and anti-coagulatory activities in diabetic mice. Food Funct. 2015;9:2967-2974.

Jahan ST, Sadat SMA, Walliser M, Haddadi A. Targeted Therapeutic Nanoparticles: An Immense Promise to Fight against Cancer. J. Drug Deliv. 2017;2017:9090325.. https://doi.org/10.1155/2017/9090325.

Jain NK. Controlled and novel drug delivery. CBS Publication. 2001;1:292-301.

Kalyanavenkataraman S, Nanjan P, Banerji A, Nair BG, Kumar GB. Discovery of arjunolic acid as a novel nonzinc binding carbonic anhydrase II inhibitor. Bioorg. Chem. 2016;66:72-79.

Kamble SM, Patil CR. Asiatic acid Ameliorates doxorubicin-induced cardiac and hepato-renal toxicities with Nrf2 transcriptional factor activation in rats. Cardiovasc. Toxicol. 2018;18:131-141.

Kamble SM, Patel HM, Goyal SN, Noolvi MN, Mahajan UB, Ojha S. In silico evidence for binding of pentacyclic triterpenoids to Keap1- Nrf2 protein-protein binding site. Comb. Chem. High Throughput Screen. 2017;20:215-234.

Kim KB, Kim K, Bae S, Choi Y, Cha HJ, Kim SY. MicroRNA- 1290 promotes asiatic acid-induced apoptosis by decreasing BCL2 protein level in A549 non-small cell lung carcinoma cells. Oncol. Rep. 2014;32:1029-1036.

Kim T, Hyeon T. Applications of inorganic nanoparticles as therapeutic agents. Nanotechnology. 2014;25(1):1-14.

Korsmeyer RW, Gurny R, Doelker E, Buri P, Peppas NA. Mechanisms of solute release from porous hydrophilic polymers. Int J Pharm. 1983;15:25-35.

Kumari A, Yadav SK, Yadav SC. Biodegradable polymeric nanoparticles based drug delivery systems. Colloids Surf B Biointerfaces. 2010;75:1-18.

Lamprecht A, Ubrich N, Hombreiro Pérez M, Lehr CM, Hoffman M, Maincent P. Biodegradable monodispersed nanoparticles prepared by pressure homogenization emulsification. Int J Pharm. 1999;184(1):97-105.

Lin W, Huang Y -W, Zhou X -D, Ma Y. In vitro toxicity of silica nanoparticles in human lung cancer cells. Toxicol. Appl. Pharmacol. 2006;217(3):252 -259.

Liu J, Chen L, Lu H. Asiatic Acid Enhances Antioxidant and Anti-inflammatory Activity to Suppress Isoproterenol Induced Cardiotoxicity. Int J Pharmacol. 2018;14(7):1038-1045.

Liu J, He T, Lu Q, Shang J, Sun H, and Zhang L. Asiatic acid preserves beta cell mass and mitigates hyperglycemia in streptozocin-induced diabetic rats. Diabetes Metab. Res. Rev. 2010;26:448-454.

Lombardo D, Mikhail A. Kiselev, Caccamo MT. Smart Nanoparticles for Drug Delivery Application: Development of Versatile Nanocarrier Platforms in Biotechnology and Nanomedicine. J Nanomater. 2019:3702518: https://doi.org/10.1155/2019/3702518.

Lv H, Qi Z, Wang S, Feng H, Deng X, Ci X. Asiatic Acid Exhibits Anti-inflammatory and Antioxidant Activities against Lipopolysaccharide and d-Galactosamine-Induced Fulminant Hepatic Failure. Front Immunol. 2017;8:785. https://doi.org/10.3389/fimmu.2017.00785.

Lv J, Sharma A, Zhang T, Wu Y, Ding X. Pharmacological Review on Asiatic Acid and Its Derivatives: A Potential Compound. SLAS TECHNOL. 2018;23(2):111-127.

Ma H, Liang X -J. Fullerenes as unique nanopharmaceuticals for disease treatment. Sci. China Chem. 2010;53(11):2233-2240.

Maji R, Dey NS, Satapathy BS, Mukherjee B, Mondal S. Preparation and characterization of tamoxifen citrate loaded nanoparticles for breast cancer therapy. Int. J. Nanomedicine. 2014;9:3107–3118.

Matsumura Y, Maeda H. A new concept for macromolecular therapeutics in cancer chemotherapy: mechanism of tumoritropic accumulation of proteins and the antitumor agent smancs. Cancer Res. 1986;46:6387-6392.

Meeran MFN, Goyal SN, Suchal K, Sharma C, Patil CR, Ojha SK. Pharmacological Properties, Molecular Mechanisms, and Pharmaceutical Development of Asiatic Acid: A Pentacyclic Triterpenoid of Therapeutic Promise. Front Pharmacol. 2018;09:1-35. doi: 10.3389/fphar.2018.00892.

Meißner T, Potthoff A, Richter V. Suspension characterization as important key for toxicological investigations. J Phys Conf Ser. 2009;170(1):012012.

Michalet X, Pinaud FF, Bentolila L. Quantum dots for live cells, in vivo imaging, and diagnostics. Science. 2005;307(5709):538-544.

Mirakabad FST, Nejati-Koshki K, Akbarzadeh A, Yamchi MR, Milani M, Zarghami N, Zeighamian V, Rahimzadeh A, Alimohammadi S, Hanifehpour Y, Joo SW. PLGA-Based Nanoparticles as Cancer Drug Delivery Systems. Asian Pac J Cancer Prev. 2014;15. http://dx.doi.org/10.7314/APJCP.2014.15.2.517.

Mishra D, Hubenak J, Mathur A. Nanoparticle systems as tools to improve drug delivery and therapeutic efficacy. J Biomed Mater Res A. 2013;101(12):1-15.

Moorthi C, Manavalan R, Kathiresan K. Nanotherapeutics to Overcome Conventional Cancer Chemotherapy Limitations. J Pharm Pharmaceut Sci. 2011;14(1):67-77.

Mukherjee B, Roy G, Santra K, Sahana B. Lactide-glycolide polymers as nanodimensional carriers for drugs. Int J Biomed Nanosci Nanotechnol. 2010;1:230-246.

Nagarkar R, Patel J. Polyvinyl Alcohol: A Comprehensive Study. ASPS. 2019;3(4):34-44.

Narvekar M, Xue HY, Eoh JY, Wong HL. Nanocarrier for poorly water-soluble anticancer drugs--barriers of translation and solutions. AAPS PharmSciTech. 2014;15(4):822-833.

Nussenbaum F, Herman IM. Tumor angiogenesis: insights and innovations. Int J Oncol. 2010. http://dx.doi.org/10.1155/2010/132641.

Orive G, Anitua E, Pedraz J, Emerich D. Biomaterials for promoting brain protection, repair and regeneration. Nat. Rev. Neurosci. 2009;10(9):682-692.

Pal SL, Jana U, Manna PK, Mohanta GP, Manavalan R. Nanoparticle: An overview of preparation and characterization. J Appl Pharm Sci. 2011; 01:228-234.

Park BC, Bosire KO, Lee ES, Lee YS, Kim JA. Asiatic acid induces apoptosis in SK-MEL-2 human melanoma cells. Cancer Lett. 2005;218:81-90.

Park TG. Degradation of poly (D, L-lactic acid) microspheres: effect of molecular weight. J Control Release. 1994;30:161-73.

Parveen S, Misra R, Sahoo S. Nanoparticles: a boon to drug delivery, therapeutics, diagnostics and imaging. Nanomedicine Nanotechnology, Biol. Med. 2012;8(2):147-166.

Patel S, Pandey G, Yadav SK. Review on nanoemulsion based drug delivery system. AJPER. 2018;7(2):17-27.

Patil KR, Mohapatra P, Patel HM, Goyal, SN, Ojha S, Kundu CN. Pentacyclic triterpenoids inhibit IKKb mediated activation of NF-kB pathway: in silico and in vitro evidences. PLoS ONE 2015;10:e0125709. http://dx.doi.org/10.1371/journal.pone.0125709.

Paul P, Sengupta S, Mukherjee B, Shaw TK, Gaonkar RH, Debnath MC. Chitosan-coated nanoparticles enhanced lung pharmacokinetic profile of voriconazole upon pulmonary delivery in mice. Nanomedicine (Lond.). 2018;13(5):501-520.

Potrony M, Badenas C, Aguilera P, Puig-Butille JA, Carrera C. Update in genetic susceptibility in melanoma. Ann. Transl. Med. 2015;15:210. http://dx.doi.org/10.3978/j.issn.2305 5839.2015.08.11.

Ramachandran V, Saravanan R. Asiatic acid prevents lipid peroxidation and improves antioxidant status in rats with streptozotocininduced diabetes. J. Funct. Foods. 2013;5:1077-1087.

Ramachandran V, Saravanan R. Glucose uptake through translocation and activation of GLUT4 in PI3K/Akt signaling pathway by asiatic acid in diabetic rats. Hum. Exp. Toxicol. 2015;34:884-893.

Ramachandran V, Saravanan R, Senthilraja P. Antidiabetic and antihyperlipidemic activity of asiatic acid in diabetic rats, role of HMG CoA: in vivo and in silico approaches. Phytomedicine. 2014;21:225-232.

Ramachandran V, Saravanan R. Asiatic acid prevents lipid peroxidation and improves antioxidant status in rats with streptozotocin-induced diabetes. J Funct Foods. 2013;5(3):1077-1087.

Rangasamy M. Nano Technology: A Review. J Appl Pharm Sci. 2011;1(2):8-16.

Ratner B, Hoffman A, Schoen F, Lemons J. Biomaterials Science: An Introduction to Materials in Medicine. Third Edit. Canada: Academic Press; 2014.

Reis C, Neufeld R, Ribeiro A, Veiga F. Nanoencapsulation I. Methods for preparation of drug-loaded polymeric nanoparticles. Nanomedicine. 2006;2(1):8-21.

Ricci MS, Zong WX. Chemotherapeutic approaches for targeting cell death pathways. Oncologist. 2006;11(4):342-357.

Rizvi SAA, Saleh AM. Applications of nanoparticle systems in drug delivery technology. Saudi Pharm J. 2018;26(1):64-70.

Roeven E, Scheres L, Smulders MMJ, Zuilhof H. design, synthesis, and characterization of fully zwitterionic, functionalized dendrimers. ACS Omega. 2019; 4(2):3000- 3011.

Rudra A, Manasadeepa R, Ghosh MK, Ghosh S, Mukherjee B. Doxorubicin-loaded phosphatidylethanolamine-conjugated nanoliposomes: *In vitro* and their accumulation in liver, kidneys, and lungs in rats. Int J Nanomedicine. 2010;5:811-823.

Santo V, Rodrigues M, Gomes M. Contributions and future perspectives on the use of magnetic nanoparticles as diagnostic and therapeutic tools in the field of regenerative medicine. Expert Rev. Mol. Diagn. 2013;13(6):553-566.

Satapathy BS, Mukherjee B, Baishya R, Debnath MC, Dey NS, Maji R. Lipid nanocarrier-based transport of docetaxel across the blood brain barrier. RSC Adv. 2016;6(88):85261-85274.

Schliecker G, Schmidt C, Fuchs S, Kissel T. Characterization of a homologous series of D, L-lactic acid oligomers; a mechanistic study on the degradation kinetics in vitro. Biomaterials. 2003;24:3835-44.

Shewach DS, Kuchta RD. Introduction to cancer chemotherapeutics. Chem Rev. 2009;109(7):2859-2861.

Si L, Xu J, Yi C, Xu X, Ma C, Yang J. Asiatic acid attenuates the progression of left ventricular hypertrophy and heart failure induced by pressure overload by Inhibiting Myocardial Remodeling in Mice. J. Cardiovasc. Pharmacol. 2015;66:558-568.

Si L, Xu J, Yi C, Xu X, Wang F, Gu W. Asiatic acid attenuates cardiac hypertrophy by blocking transforming growth factor-b1- mediated hypertrophic signaling in vitro and in vivo. Int. J. Mol. Med. 2014;34:499–506.

Siepmann J, Peppas NA. Modeling of drug release from delivery systems based on hydroxypropyl methylcellulose (HPMC). Adv. Drug Deliv. Rev. 2001;48:139-157.

Sindhura Reddy N, Sowmya S, Bumgardner JD, Chennazhi KP, Biswas R, Jayakumar R. Tetracycline nanoparticles loaded calcium sulfate composite beads for periodontal management. Biochim. Biophys. Acta Gen. Subj. 2014;1840:2080-2090.

Singh R, Lillard JW Jr. Nanoparticle-based targeted drug delivery. Exp Mol Pathol. 2009;86(3):215-223.

Sinha B, Mukherjee B, Pattnaik G. Poly-lactide-co-glycolide nanoparticles containing voriconazole for pulmonary delivery: *In vitro* and *in vivo* study. Nanomedicine. 2013;9 (1):94-104.

Slotkin J, Chakrabarti L, Dai H. In vivo quantum dot labelling of mammalian stem and progenitor cells. Dev. Dyn. 2009;236(12):3393-3401.

Steelman LS, Chappell WH, Abrams SL, Kempf RC, Long J, Laidler P. Roles of the Raf/MEK/ERK and PI3K/PTEN/Akt/mTOR pathways in controlling growth and sensitivity to therapy-implications for cancer and aging. Aging. 2011;3:192-222.

Sun SB, Liu P, Shao FM, Miao QL. Formulation and evaluation of PLGA nanoparticles loaded capecitabine for prostate cancer. Int. J. Clin. Exp. Med. 2015;8(10):19670-19681.

Sun W, Xu G, Guo X. Protective effects of asiatic acid in a spontaneous type 2 diabetic mouse model. Mol Med Rep. 2017;16(2):1333-1339.

Sutradhar KB, Amin ML. Nanotechnology in Cancer Drug Delivery and Selective Targeting. ISRN Nanotechnology. 2014; 939378.

Tran S, DeGiovanni PJ, Piel B, Rai P. Cancer nanomedicine: a review of recent success in drug delivery. Clin Transl Med. 2017;6(1):44. doi:10.1186/s40169-017-0175-0.

Vueba ML, Batista de Carvalho LA, Veiga F, Sousa JJ, Pina ME. Influence of cellulose ether polymers on ketoprofen release from hydrophilic matrix tablets. Eur J Pharm Biopharm. 2004;58(1):51-59.

Wakaskar RR. Passive and active targeting in tumor microenvironment. Int. J. Drug Dev. Res. 2017;9(2):37-41.

Wang L, Xu J, Zhao C, Zhao L, Feng B. Antiproliferative, cell-cycle dysregulation effects of novel asiatic acid derivatives on human non-small cell lung cancer cells. Chem. Pharm. Bull. 2013;61:1015–1023. Wang X, Lu Q, Yu DS, Chen YP, Shang J, Zhang LY. Asiatic acid mitigates hyperglycemia and reduces islet fibrosis in Goto-Kakizaki rat, a spontaneous type 2 diabetic animal model. Chinese J. Nat. Med. 2015;13:529–534.

Wen X, Sun H, Liu J, Cheng K, Zhang P, Zhang L. Naturally occurring pentacyclic triterpenes as inhibitors of glycogen phosphorylase: synthesis, structure-activity relationships, and X-ray crystallographic studies. J. Med. Chem. 2008;51:3540-3554.

Wen X, Sun H, Liu J, Cheng K, Zhang P, Zhang L. Naturally occurring pentacyclic triterpenes as inhibitors of glycogen phosphorylase: synthesis, structure-activity relationships, and X-ray crystallographic studies. J. Med. Chem. 2008;51:3540-3554.

Xu X, Si L, Xu J, Chenlong Y, Wang F, Gu W. Asiatic acid inhibits cardiac hypertrophy by blocking interleukin-1b-activated nuclear factor-kB signaling in vitro and in vivo. J. Thorac. Dis. 2015;10:1787–1797.

Yoshida M, Fuchigami M, Nagao T, Okabe H, Matsunaga K. Antiproliferative constituents from Umbelliferae plants VII. Active triterpenes and rosmarinic acid from C. asiatica. Biol. Pharm. Bull. 2005;28:173-175.

Yu DH, Lu Q, Xie J, Fang C, Chen HZ. Peptide-conjugated biodegradable nanoparticles as a carrier to target paclitaxel to tumor neovasculature. Biomaterials. 2010;31(8):2278–2292.

Zalcman GE, Bergot E, Lechapt E. Update on non-small cell lung cancer. Eur. Respir. Rev. 2010;19:173-185.

Zhao YL, Wei H, Zheng HH, Guo Z, Wei YS, Zhang DH, Zhang J. Enhancing water-solubility of poorly soluble drug, asiatic acid with hydroxypropyl-β-cyclodextrin. Dig J Nanomater Bios. 2010;5(2):419-425.

Web References

https://www.microscopemaster.com/nanotherapy.html, viewed on April 5, 2019.

https://www.cif.iastate.edu/nmr/nmr-tutorials/sample-preparation, viewed on May 10, 2019.